SN 2008in—BRIDGING THE GAP BETWEEN NORMAL AND FAINT SUPERNOVAE OF TYPE IIP

Rupak Roy[1], Brijesh Kumar[1], Stefano Benetti[2], Andrea Pastorello[3], Fang Yuan[4,5], Peter J. Brown[6],
Stefan Immler[7,8], Timur A. Fatkhullin[9], Alexander S. Moskvitin[9], Justyn Maund[10], Carl W. Akerlof[4],
J. Craig Wheeler[11], Vladimir V. Sokolov[9], Rorbert M. Quimby[12], Filomena Bufano[2], Brajesh Kumar[1,13],
Kuntal Misra[14,15], S. B. Pandey[1,4], Nancy Elias-Rosa[16], Peter W. A. Roming[17], and Ram Sagar[1]
[1] Aryabhatta Research Institute of Observational Sciences (ARIES), Manora Peak, Nainital 263 129, India; roy@aries.res.in, rupakroy1980@gmail.com
[2] Istituto Nazionale di Astrofisica, Observatorio Astronomico di Padova, Italy
[3] Astrophysics Research Centre, School of Mathematics and Physics, Queen's University Belfast, Belfast BT7 1NN, UK
[4] Randall Laboratory of Physics, University of Michigan, 450 Church Street, Ann Arbor, MI 48109-1040, USA
[5] Research School of Astronomy and Astrophysics, The Australian National University, Cotter Road, Weston Creek, ACT 2611, Australia
[6] Department of Physics and Astronomy, University of Utah, Salt Lake City, UT 84112, USA
[7] NASA/Goddard Space Flight Center, Astrophysics Science Division, Code 662, Greenbelt, MD 20771, USA
[8] Department of Astronomy, University of Maryland, College Park, MD 20742, USA
[9] Special Astrophysical Observatory, Nizhnij Arkhyz, Karachaevo-Cherkesia 369167, Russia
[10] Dark Cosmology Centre, Niels Bohr Institute, University of Copenhagen, Juliane Maries Vej 30, 2100 Copenhagen, Denmark
[11] Department of Astronomy, University of Texas, Austin, TX 787120259, USA
[12] Cahill Center for Astrophysics, California Institute of Technology, Pasadena, CA 91125, USA
[13] Institut d'Astrophysique et de Géophysique, Université de Liège, Allée du 6 Août 17, Bât B5c, 4000 Liège, Belgium
[14] Space Telescope Science Institute, 3700 San Martin Drive, Baltimore, MD 21218, USA
[15] Inter University Center for Astronomy and Astrophysics, Post Bag 4, Ganeshkhind, Pune 411 007, India
[16] Institut de Ciències de L'Espai (IEEC-CSIC), Campus UAB, 08193 Bellaterra, Spain
[17] Space Science and Engineering Division, 6220 Culebra Rd, San Antonio, TX 78238-5166, USA

ABSTRACT

We present optical photometric and low-resolution spectroscopic observations of the Type II plateau supernova (SN) 2008in, which occurred in the outskirts of the nearly face-on spiral galaxy M61. Photometric data in the X-ray, ultraviolet, and near-infrared bands have been used to characterize this event. The SN field was imaged with the ROTSE-IIIb optical telescope about seven days before the explosion. This allowed us to constrain the epoch of the shock breakout to $JD = 2454825.6$. The duration of the plateau phase, as derived from the photometric monitoring, was ~ 98 days. The spectra of SN 2008in show a striking resemblance to those of the archetypal low-luminosity IIP SNe 1997D and 1999br. A comparison of ejecta kinematics of SN 2008in with the hydrodynamical simulations of Type IIP SNe by Dessart et al. indicates that it is a less energetic event ($\sim 5 \times 10^{50}$ erg). However, the light curve indicates that the production of radioactive ^{56}Ni is significantly higher than that in the low-luminosity SNe. Adopting an interstellar absorption along the SN direction of $A_V \sim 0.3$ mag and a distance of 13.2 Mpc, we estimated a synthesized ^{56}Ni mass of $\sim 0.015\ M_\odot$. Employing semi-analytical formulae derived by Litvinova and Nadezhin, we derived a pre-SN radius of $\sim 126\ R_\odot$, an explosion energy of $\sim 5.4 \times 10^{50}$ erg, and a total ejected mass of $\sim 16.7\ M_\odot$. The latter indicates that the zero-age main-sequence mass of the progenitor did not exceed 20 $M_\odot$. Considering the above properties of SN 2008in and its occurrence in a region of sub-solar metallicity ([O/H] $\sim$ 8.44 dex), it is unlikely that fall-back of the ejecta onto a newly formed black hole occurred in SN 2008in. We therefore favor a low-energy explosion scenario of a relatively compact, moderate-mass progenitor star that generates a neutron star.

Key words: supernovae: general – supernovae: individual (2008in)

Online-only material: color figures

1. INTRODUCTION

Core-collapse Type II supernovae (SNe) mark the violent death of stars with main-sequence masses greater than 8 $M_\odot$, and as is indicated by the presence of hydrogen lines in their optical spectra, they originate from a progenitor star with a significant amount of hydrogen still intact (Eldridge & Tout 2004). Of special interest are the Type II plateau SNe which are characterized by a "plateau" in their optical light curve and are more common, constituting about 75% of all Type II SNe (Smith et al. 2010). The IIP SNe show a wide range of plateau luminosities, plateau durations, expansion velocities, and nickel masses (Hamuy 2003), and these observational properties are connected with the explosion mechanism as well as the physical properties of the progenitor star such as ejected mass, explosion energy, and pre-SN radius (Nadyozhin 2003; Smartt et al. 2009). The IIP SNe are thought to result from progenitor masses in the range 8–25 $M_\odot$ (Heger et al. 2003) with an extended hydrogen envelope necessary to maintain the plateau phase. A detailed study of optical light curves and spectra of only a few nearby IIP SNe has been done so far and there exists a discrepancy in estimating the mass of their progenitors, e.g., for the three well-studied events (namely, 1999em, 2005cs, and 2004et), the determination of progenitor mass from the hydrodynamical modeling of their light curve is found to be higher than that estimated from pre-SN imaging (Utrobin et al. 2010; Bersten et al. 2011).

Recently, a number of "low-luminosity" Type IIP events have been discovered, viz., SNe 1999br, 1999eu, 1994N, 2001dc, 2005cs (Pastorello et al. 2004, 2009), 2008bk (Van Dyk et al.

2010), and 2009md (Fraser et al. 2010). These events have explosion energy ($\sim 10^{50}$ erg) and ejected ^{56}Ni mass (2–$7 \times 10^{-3} M_\odot$) both lower by a factor of 10 than normal, and low expansion velocity ~ 1000 km s^{-1} (Pastorello et al. 2009 and references therein). The low-luminosity IIP SNe are debated because of the unknown nature of their progenitors. The first reported faint SN was SN 1997D (Turatto et al. 1998; Benetti et al. 2001), and the observed properties of its light curves and spectra were explained in terms of significant fall-back of ejected material on a newly formed black hole (BH), created through the core-collapse of a massive progenitor ($M \gtrsim 20 M_\odot$; Zampieri et al. 1998, 2003). Alternatively, SN 1997D was interpreted as the explosion of a less massive progenitor (8–12 $M_\odot$; Chugai & Utrobin 2000), close in mass to the lower limit for stars that can undergo core-collapse. Heger et al. (2003) suggested that low-luminosity Type IIP events are electron capture SNe produced by low-mass progenitors giving rise to ONeMg cores. This is further supported through investigations of pre-explosion images (Maund & Smartt 2005; Maund et al. 2005), though Eldridge et al. (2007) have ruled out the possibility of such a mechanism for the low-luminosity SN 2005cs. According to the formalism of Heger et al. (2003) and Eldridge & Tout (2004), no star having initial mass less than 22 $M_\odot$ can form a BH, which can quench the ejected material and produce a low-luminosity SN. Stars with masses above 25 $M_\odot$, formed in metal-poor or slightly sub-solar metallicity regions, can produce low-luminosity, BH-forming Type IIP SNe. Type IIL/b events can be produced through this process from stars having masses >25 $M_\odot$ and generated in regions with solar (or super-solar) metallicity. So, the metallicity information at the SN location and the estimation of the initial mass are essential to constrain the triggering mechanisms of these explosions.

SN 2008in was discovered in the nearby galaxy M61 (NGC 4303). The first unfiltered CCD images of SN 2008in were taken by Koichi Itagaki on 2008 December 26.79 (all times in UT hereafter) and 27.69 at a magnitude of 14.9. Independent observations of this event by K. Kadota showed the transient at an unfiltered mag of 15.1. In addition, W. Wells recorded the SN on 2008 December 28.46 at V- and R-band magnitudes of 14.3 and 13.2, respectively (Nakano et al. 2008). Low- and mid-resolution spectroscopic observations indicate an early discovery for SN 2008in (within 1–2 weeks after core-collapse). The spectra showed highly blueshifted Hα and Hβ absorptions (by ~ 9000 km s^{-1}) with weaker emission components (Chakraborti et al. 2008; Foley 2008; Stritzinger 2008). The presence of prominent P-Cygni profiles of Balmer lines leads to its classification as a Type II SN.

The broadband light curve and the initial spectral evolution of SN 2008in were similar to those of normal Type IIP SNe. However, from mid-plateau, the SN started to show a few spectral features (like Hα) which are similar to underluminous events. SN 2008in was also observed in the radio with the Very Large Array (VLA) on 2008 December 31.40 UT in two frequency bands at 8.4601 and 22.4601 GHz (Stockdale et al. 2008). Observation for the second epoch was further reported by Stockdale et al. (2009) on 2009 January 27. Interacting Type II SNe, like Type IIn events and a few Type IIP events (e.g., SN 2004et), are supposed to be strong sources of radio emission (for review see Weiler et al. 2002). However, both VLA observations produced null results for this proximate event.

In this paper, we present optical and near-infrared photometric and optical spectroscopic observations of SN 2008in. The photometric data cover a time span of about 410 days since the discovery. The *Swift*/XRT (Burrows et al. 2005) and *Swift*/UVOT (Roming et al. 2005) data covering a time span of 60 days are also presented. In Sections 3 and 4, we study the photometric and spectroscopic evolutions, respectively. In Sections 5 and 6, we cover the estimates of distance, reddening, intrinsic color, and bolometric fluxes. The main physical parameters of the explosion and the mass of the progenitor are derived in Section 7 while a comparison of its properties with other SNe is given in Section 8. The conclusion of the paper is given in the last section. The epoch of explosion JD = 2454825.6 (Section 3) is considered throughout the paper and the times of pre-/post-explosion are denoted by $-$/+ signs, respectively.

2. OBSERVATION AND DATA REDUCTION

2.1. Photometric Observation

The prompt follow-up of the event was carried out by the ground-based ROTSE-IIIb telescope[18] having sensitivity in the wavelength region from 0.35 to 1.0 μm with a peak around 0.6 μm (Quimby et al. 2007). The SN was first detected in the ROTSE-IIIb images on 2008 December 24.45 and it was monitored at 58 phases until +115 days. The initial detections of the SN evaded the automated pipeline identification due to poor image quality and low signal-to-noise ratio (S/N). The data reduction was performed afresh on all the available ROTSE data. In order to remove the contamination of the true SN flux from the underlying galaxy, a pre-SN galaxy template was constructed from images taken in early 2008 and each SN frame was reduced using the galaxy-template subtraction scheme developed by Alard (2000). The point-spread function (PSF) photometry was performed at the SN location in the galaxy-template-subtracted images. The unfiltered instrumental magnitudes were calibrated using the USNO B1.0 R-band magnitudes of about 15 isolated stars. The light curve thus produced was found to be 0.15 mag off from the Cousins R-band light curve produced by multi-band observation carried out at ARIES (described below) and the ROTSE magnitudes were scaled accordingly.

The SN 2008in was also monitored with the Ultraviolet Optical Telescope (UVOT) on board *Swift* from +5 days to +60 days. The UVOT filters $uvw2$, $uvm2$, $uvw1$, u, b, and v have their effective wavelengths at 2030, 2231, 2634, 3501, 4329, and 5402 Å, respectively (Poole et al. 2008). The UVOT data reduction was performed following the prescriptions of Brown (2009). A 5$''$ aperture is used to measure the counts for the coincidence loss correction whereas a 3$''$ aperture was used for the photometry. For the filters $uvw2$, $uvm2$, and $uvw1$, the last epoch (obtained about 60 days after explosion when the UV flux was very weak) data were used to subtract the galaxy light, while in the optical the SN remains much brighter than the underlying light so contamination was negligible. An aperture correction (based on an average PSF in *Swift* CALDB) as well as zero points from Poole et al. (2008) was applied to put the magnitudes on the UVOT photometric system. The UVOT magnitudes are listed in Table 1.

From +5 days to +416 days, the follow-up of SN 2008in in optical broadband Johnson *UBV* and Cousins *RI* was performed

---

[18] The Robotic Optical Transient Search Experiment (ROTSE-III) is a set of four 45 cm fully robotic optical telescopes, installed at Siding Spring Observatory, Australia (ROTSE-IIIa), McDonald Observatory, Texas (ROTSE-IIIb), H.E.S.S. site, Namibia (ROTSE-IIIc), and TUBITAK National Observatory, Turkey (ROTSE-IIId; Akerlof et al. 2003; Yuan 2010).

Table 1
The *Swift*/UVOT Photometric Observations of SN 2008in

UT Date (yy/mm/dd)	JD 2454000+	Phase[a] (day)	*uvw*2 (mag)	*uvm*2 (mag)	*uvw*1 (mag)	*u* (mag)	*b* (mag)	*v* (mag)
2008/12/30.08	830.58	5.00	14.97 ± 0.05	14.65 ± 0.04	14.45 ± 0.05	14.12 ± 0.04	15.24 ± 0.04	15.20 ± 0.04
2008/12/30.60	831.11	5.53	15.13 ± 0.05	14.85 ± 0.04	14.54 ± 0.04	14.16 ± 0.04	15.20 ± 0.04	15.13 ± 0.05
2008/12/31.96	832.46	6.88	15.53 ± 0.05	15.28 ± 0.09	14.84 ± 0.05	14.32 ± 0.04	15.25 ± 0.04	15.15 ± 0.06
2009/01/01.83	833.30	7.72	15.72 ± 0.05	15.47 ± 0.05	15.01 ± 0.05	14.34 ± 0.04	15.30 ± 0.04	15.17 ± 0.04
2009/01/03.54	835.05	9.47	16.23 ± 0.05	16.07 ± 0.05	15.51 ± 0.05	14.52 ± 0.04	15.35 ± 0.04	15.25 ± 0.04
2009/01/07.79	839.29	13.71	17.87 ± 0.08	17.88 ± 0.11	16.96 ± 0.07	15.15 ± 0.04	15.49 ± 0.04	15.25 ± 0.05
2009/01/11.15	842.64	17.06	18.81 ± 0.11	18.66 ± 0.14	17.80 ± 0.09	15.74 ± 0.04	15.62 ± 0.04	15.27 ± 0.04
2009/01/19.79	851.30	25.72	. . .	. . .	18.67 ± 0.16	16.67 ± 0.05	16.00 ± 0.04	15.36 ± 0.05
2009/01/22.00	884.53	58.95	. . .	. . .	. . .	17.92 ± 0.07	16.77 ± 0.05	15.69 ± 0.04
2009/01/22.73	885.23	59.65	. . .	. . .	. . .	18.02 ± 0.09	16.75 ± 0.05	15.68 ± 0.05

Note. [a] With reference to the explosion epoch JD 2454825.6.

with the 1 m Sampurnanand Telescope (ST) at ARIES, Naini-tal.[19] An identification chart showing the field of the galaxy M61 along with the locations of SN 2008in as well as the local standards is presented in Figure 1. The photometry is performed using standard tasks of IRAF[20] and *DAOPHOT*[21] as described in the paper by Roy et al. (2011). Bias subtraction and flat fielding were performed on the raw frames and the cosmic removal was done using the LACOSMIC routine (van Dokkum 2001). As the SN lies in the outskirts of the galaxy on a relatively faint and smooth background, the photometry at the initial phases (mostly during the plateau phase when the SN is bright) is estimated using the profile fitting method. During nebular phases, when the SN becomes faint, the true SN flux is estimated using the galaxy template subtraction method following the procedures of Roy et al. (2011). As a galaxy template, we used post-explosion (+600 days) images observed on 2011 January 4 under good seeing conditions. Figure 2 shows an example of this procedure applied to a late-time *V*-band image of SN 2008in. In the template image of 2011 January 4, we can see a clear flux enhancement located approximately 5″ away (a linear distance of ∼343 pc) from the SN position. This knot is also present in a deep image from the Sloan Digital Sky Survey (SDSS) and it is identified as a H II region in the NED catalog. The progenitor of SN 2008in may have a possible association with this star-forming region. The field of SN 2008in was calibrated using Landolt (2009) standard stars of the field SA98 observed on the same night as the SN. A sample of 10 bright and isolated non-variable stars in the field of SN 2008in was used as local standards to derive the zero points for the SN at each epoch. The location and magnitudes of these local standards are listed in Table 2. The entire time span of photometric observation is about 410 days, and in Table 3 we report the *UBVRI* photometry of the event.

From +4 days to +116 days, the SN 2008in was also observed in *JHK* near-infrared (NIR) bands with the 0.6 m REM/REMIR at La Silla (Zerbi et al. 2004). The object was clearly visible

in the *J* and *H* passbands, while it remained undetected in *K*. The instrumental magnitudes were standardized using the Two Micron All Sky Survey standards available in the field of SN 2008in. The calibrated *JH* magnitudes are listed in Table 4.

2.2. X-ray Observations

The *Swift* XRT observations were obtained simultaneously with the UVOT observations. To search for X-ray emission from SN 2008in, we extracted X-ray counts from a circular region with a 10 pixel radius (23″.7; corresponding to the XRT on-axis 90% encircled energy radius) centered on the optical position of the SN. The background was extracted locally from a source-free region of 40″ radius to account for the detector, sky background, and the diffuse emission from the host galaxy.

No X-ray source is detected in the merged 27.1 ks XRT data obtained in photon-counting mode. The 3σ upper limit to the XRT net count rate is 7.2×10^{-4} counts s^{-1}, corresponding to an unabsorbed (0.2–10 keV band) X-ray flux of $f_{0.2-10} < 3.4 \times 10^{-14}$ erg cm^{-2} s^{-1} and a luminosity of $L_{0.2-10} < 7.0 \times 10^{38}$ erg s^{-1} for an adopted thermal plasma spectrum with a temperature of $kT = 10$ keV (see Fransson et al. 1996 and references therein), a Galactic foreground column density of $N_{\rm H} = 1.67 \times 10^{20}$ cm^{-2} (Dickey & Lockman 1990), and a distance of 13.19 Mpc (Section 5).

2.3. Optical Spectroscopic Observation

Long-slit low-resolution spectra (∼6 to 14 Å) in the optical range (0.33–1.0 µm) were collected at 11 phases from +7 days to +143 days, including five phases from the 2 m IGO, three phases from the 9.2 m HET, two phases from the 6 m BTA, and one epoch from the 3.6 m NTT.[22] A journal of spectroscopic observations is given in Table 5. The spectroscopic data acquired from IGO, NTT, and HET were reduced under the IRAF environment. Bias and flat-fielding were performed on all the frames. Cosmic-ray rejection was done using the Laplacian kernel detection method (van Dokkum 2001). All the data obtained from the BTA were reduced using programs in the IDL software environment.

The instrumental FWHM resolution of 2 m IGO spectra as measured from the [O I] λ5577 emission skyline was found to lie between 6 and 10 Å (∼322–510 km s^{-1}). Flux calibration was done using standard spectrophotometric fluxes from Hamuy et al. (1994), assuming a mean extinction for the site. For HET,

---

[19] A 2048 × 2048 CCD camera mounted at the f/13 Cassegrain focus of the telescope has a square pixel of 24 µm on a side, and with a plate scale of 0.38 arcsec per pixel, it covers a square area of 13′ on a side in the sky. The gain and readout noise of the CCD camera are 10 electrons per analog-to-digital unit and 5.3 electrons, respectively. To improve the S/N and optimize the sampling, the observations were carried out in a binned mode of 2 × 2 pixel.

[20] IRAF stands for Image Reduction and Analysis Facility distributed by the National Optical Astronomy Observatory which is operated by the Association of Universities for Research in Astronomy, Inc., under cooperative agreement with the National Science Foundation.

[21] *DAOPHOT* stands for Dominion Astrophysical Observatory Photometry (Stetson 1987).

[22] The full names of the telescope are provided in Table 5.
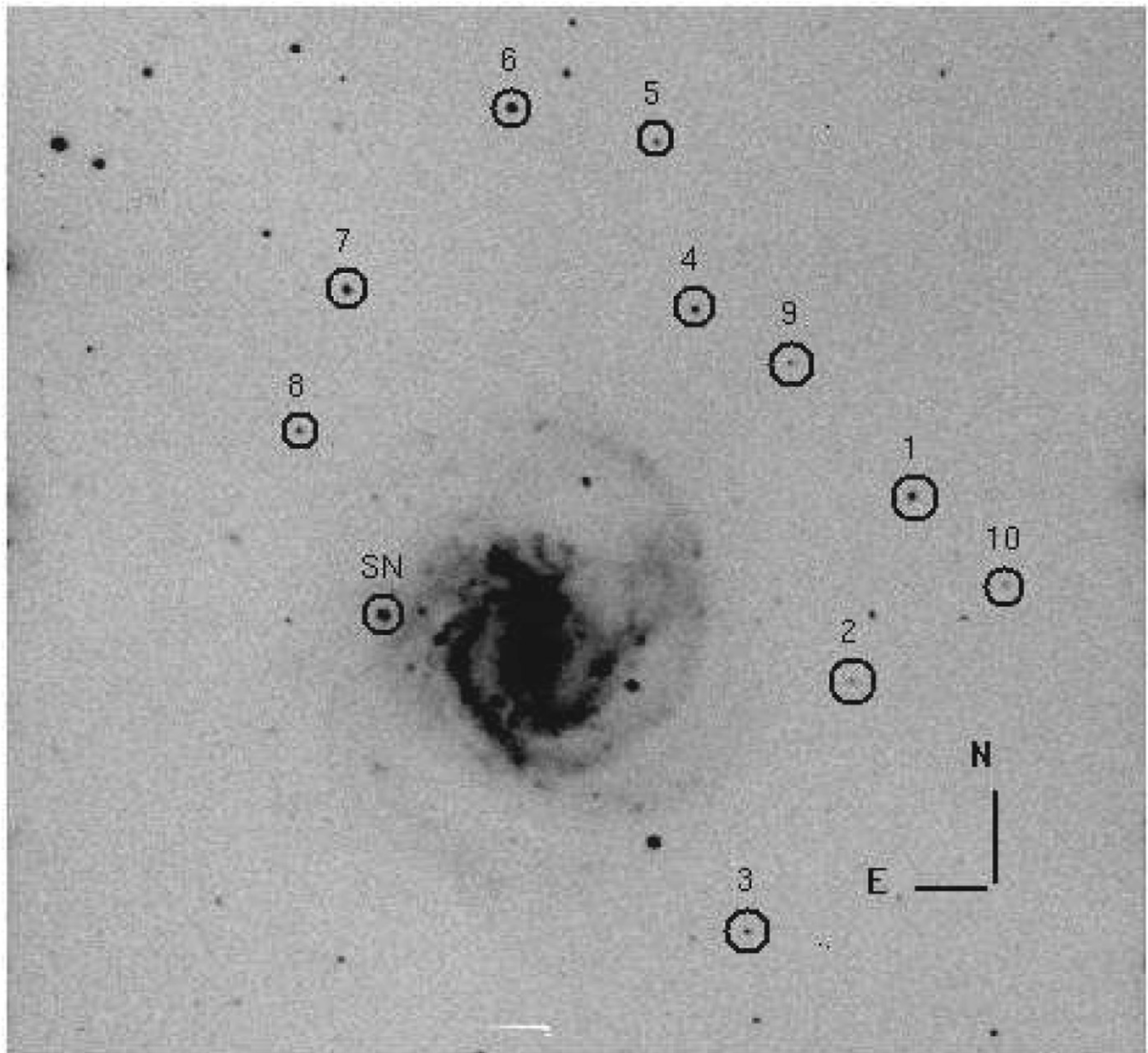
Figure 1. SN 2008in in M61. A 600 s V-band image taken at phase +32 days from the 1 m ST ARIES, India and covering an area of about $10' \times 10'$ is shown. The location of SN 2008in and the local standard stars are marked with circles. North is up and east is to the left.

Table 2
The Photometric Magnitudes of Secondary Standard Stars in the Field of SN 2008in

Star ID	α_{J2000} (h m s)	δ_{J2000} (° ′ ″)	U (mag)	B (mag)	V (mag)	R (mag)	I (mag)
1	12 21 38	04 30 26	16.99 ± 0.03	17.69 ± 0.03	17.33 ± 0.05	16.96 ± 0.06	16.59 ± 0.05
2	12 21 40	04 28 18	$\ldots$	19.49 ± 0.05	18.38 ± 0.04	17.85 ± 0.01	17.40 ± 0.02
3	12 21 44	04 25 24	17.91 ± 0.04	18.09 ± 0.02	17.65 ± 0.01	17.30 ± 0.02	16.94 ± 0.01
4	12 21 48	04 32 27	18.38 ± 0.11	17.61 ± 0.01	16.02 ± 0.01	15.10 ± 0.01	14.34 ± 0.01
5	12 21 50	04 34 20	19.10 ± 0.21	18.45 ± 0.04	17.25 ± 0.01	16.55 ± 0.01	15.99 ± 0.01
6	12 21 57	04 34 38	16.06 ± 0.01	15.72 ± 0.00	14.88 ± 0.00	14.36 ± 0.01	13.94 ± 0.00
7	12 22 04	04 32 30	16.66 ± 0.02	16.30 ± 0.00	15.48 ± 0.01	15.00 ± 0.01	14.61 ± 0.01
8	12 22 05	04 30 51	18.05 ± 0.06	18.17 ± 0.01	17.60 ± 0.04	17.25 ± 0.03	16.93 ± 0.01
9	12 21 43	04 31 54	19.56 ± 0.41	19.20 ± 0.05	17.55 ± 0.01	16.53 ± 0.01	15.51 ± 0.01
10	12 21 33	04 29 29	19.11 ± 0.43	18.96 ± 0.02	18.55 ± 0.02	18.21 ± 0.05	17.89 ± 0.02

Note. Errors in magnitude represent rms scatter of the night-to-night repeatability over the entire period of SN monitoring.
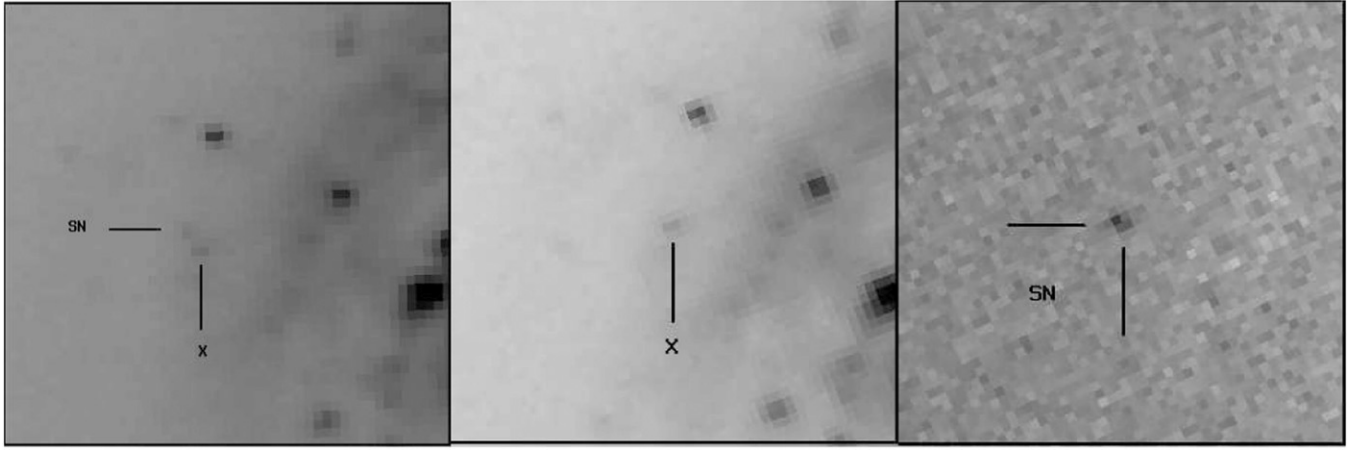
Figure 2. Measurement procedure of the true SN flux in the nebular phase. Each image shows $76'' \times 76''$ around the SN location. North is up and east is to the left. The leftmost panel shows the V-band image observed on 2010 January 20 with an SN in it. The middle panel shows the template image taken on 2011 January 4, with no SN in it. A small flux enhancement marked with a cross ("×") symbol is probably due to a star-forming region. The rightmost panel shows the subtracted image, where only an SN is present.

Table 3
The *UBVRI* Photometry of SN 2008in

UT Date (yy/mm/dd)	JD 2454000+	Phase[a] (day)	U (mag)	B (mag)	V (mag)	R (mag)	I (mag)	Seeing[b] ('')
2008/12/30.00	830.50	+5	14.23 ± 0.01	15.33 ± 0.01	15.07 ± 0.01	14.86 ± 0.01	14.86 ± 0.01	2.9
2009/01/01.98	833.48	+8	14.39 ± 0.01	15.54 ± 0.01	15.17 ± 0.01	14.65 ± 0.01	14.98 ± 0.01	1.3
2009/01/09.02	840.52	+15	15.47 ± 0.02	15.76 ± 0.02	15.21 ± 0.02	14.89 ± 0.02	14.87 ± 0.03	2.5
2009/01/23.95	855.45	+30	16.85 ± 0.04	16.36 ± 0.01	15.38 ± 0.02	15.00 ± 0.01	14.85 ± 0.01	2.1
2009/01/26.02	857.52	+32	16.90 ± 0.04	16.41 ± 0.02	15.39 ± 0.01	14.98 ± 0.01	14.85 ± 0.02	3.1
2009/01/27.01	858.33	+33	16.81 ± 0.02	16.41 ± 0.01	15.39 ± 0.01	15.00 ± 0.01	14.83 ± 0.01	2.8
2009/01/28.83	860.33	+35	16.83 ± 0.03	16.48 ± 0.01	15.43 ± 0.01	15.04 ± 0.01	14.89 ± 0.01	2.2
2009/01/30.88	862.38	+37	17.16 ± 0.04	16.53 ± 0.01	15.43 ± 0.01	15.02 ± 0.01	14.85 ± 0.01	2.4
2009/02/02.89	864.39	+39	17.11 ± 0.04	16.53 ± 0.01	15.42 ± 0.01	14.99 ± 0.01	14.78 ± 0.01	2.0
2009/02/15.82	878.32	+53	17.58 ± 0.05	16.87 ± 0.01	15.43 ± 0.02	14.76 ± 0.01	14.82 ± 0.01	2.8
2009/02/16.96	879.46	+54	17.74 ± 0.06	16.84 ± 0.01	15.54 ± 0.01	15.09 ± 0.02	14.83 ± 0.01	3.1
2009/02/17.79	880.29	+55	17.79 ± 0.05	16.87 ± 0.01	15.55 ± 0.01	15.10 ± 0.02	14.85 ± 0.01	3.1
2009/02/20.87	883.37	+58	17.92 ± 0.07	16.94 ± 0.01	15.59 ± 0.02	15.09 ± 0.01	14.84 ± 0.01	3.1
2009/02/23.77	886.27	+61	18.05 ± 0.04	17.08 ± 0.01	. . .	15.13 ± 0.01	14.89 ± 0.01	3.1
2009/02/25.81	888.31	+63	18.13 ± 0.05	17.05 ± 0.01	15.60 ± 0.01	15.14 ± 0.01	14.92 ± 0.01	2.9
2009/02/26.80	889.30	+64	. . .	. . .	15.62 ± 0.01	15.15 ± 0.01	. . .	3.8
2009/03/02.78	893.28	+68	. . .	17.08 ± 0.01	15.63 ± 0.01	15.17 ± 0.01	14.90 ± 0.00	4.4
2009/03/04.77	895.27	+70	. . .	17.15 ± 0.01	15.66 ± 0.01	15.18 ± 0.01	14.94 ± 0.01	2.4
2009/03/09.76	900.27	+75	18.72 ± 0.14	17.31 ± 0.02	15.68 ± 0.01	. . .	15.08 ± 0.01	2.3
2009/03/15.27	905.77	+80	. . .	17.20 ± 0.02	. . .	15.21 ± 0.01	14.92 ± 0.01	2.2
2009/03/24.80	915.30	+90	18.73 ± 0.08	17.42 ± 0.01	15.94 ± 0.01	15.48 ± 0.01	15.15 ± 0.01	2.5
2009/04/03.75	925.25	+100	19.28 ± 0.15	17.66 ± 0.02	16.10 ± 0.01	15.57 ± 0.01	15.31 ± 0.01	2.2
2009/04/05.61	927.22	+102	. . .	. . .	. . .	15.67 ± 0.01	15.41 ± 0.01	2.5
2009/04/10.67	932.33	+107	. . .	18.38 ± 0.06	16.76 ± 0.01	16.20 ± 0.01	15.84 ± 0.02	2.7
2009/04/17.60	939.25	+114	. . .	19.83 ± 0.06	17.91 ± 0.01	17.13 ± 0.01	16.68 ± 0.01	2.8
2009/04/22.68	944.11	+118	. . .	20.30 ± 0.16	18.10 ± 0.03	17.21 ± 0.03	16.85 ± 0.04	3.5
2009/04/28.71	950.17	+125	. . .	20.40 ± 0.09	. . .	17.24 ± 0.01	16.74 ± 0.01	2.2
2009/05/01.72	953.10	+127	. . .	20.22 ± 0.11	18.06 ± 0.04	17.27 ± 0.04	16.70 ± 0.04	2.7
2009/05/23.69	975.18	+150	. . .	. . .	18.30 ± 0.04	17.47 ± 0.02	17.00 ± 0.03	2.7
2009/05/25.70	977.21	+152	. . .	20.21 ± 0.12	18.35 ± 0.02	17.45 ± 0.01	. . .	2.6
2009/05/26.71	978.22	+153	. . .	20.15 ± 0.17	18.33 ± 0.04	17.49 ± 0.02	17.06 ± 0.03	2.8
2009/06/14.69	997.19	+172	. . .	. . .	18.39 ± 0.04	. . .	. . .	2.9
2010/01/17.98	1214.49	+389	. . .	. . .	. . .	19.69 ± 0.07	19.27 ± 0.13	1.9
2010/01/19.91	1216.42	+391	. . .	21.47 ± 0.12	20.34 ± 0.05	19.76 ± 0.05	19.52 ± 0.07	2.3
2010/02/13.91	1241.42	+416	. . .	. . .	20.57 ± 0.07	19.77 ± 0.06	. . .	2.2

Notes. The photometric observations are taken with the 1 m ST, ARIES, Nainital. Errors in magnitude denote 1σ uncertainty.
[a] With reference to the explosion epoch JD 2454825.6.
[b] FWHM of the stellar PSF at the V band. The nights for which we do not have any observation in the V band, PSF is found through interpolation.

5

Table 4
The REM Near-infrared Observation of SN 2008in

UT Date (yy/mm/dd)	JD 2454000+	Phase[a] (day)	J (mag)	H (mag)
2008/12/29.85	830.36	4.78	14.66 ± 0.054	14.55 ± 0.064
2009/01/03.87	835.37	9.78	14.60 ± 0.077	14.38 ± 0.058
2009/01/09.73	841.23	15.65	14.39 ± 0.059	14.16 ± 0.072
2009/01/14.73	846.23	20.65	14.47 ± 0.107	14.32 ± 0.150
2009/01/19.78	851.24	25.66	14.54 ± 0.150	...
2009/01/24.76	856.26	30.67	14.25 ± 0.077	14.11 ± 0.087
2009/01/29.87	861.37	35.79	14.37 ± 0.050	14.14 ± 0.065
2009/02/05.66	868.16	42.58	14.43 ± 0.067	14.24 ± 0.107
2009/02/11.69	874.19	48.61	14.20 ± 0.107	14.59 ± 0.241
2009/02/16.72	879.22	53.64	14.43 ± 0.050	14.35 ± 0.097
2009/02/21.75	884.25	58.67	...	14.18 ± 0.063
2009/02/27.75	890.25	64.67	...	14.44 ± 0.077
2009/03/04.89	895.40	69.82	14.40 ± 0.074	14.12 ± 0.085
2009/03/10.74	901.24	75.66	...	14.36 ± 0.190
2009/03/21.71	912.21	86.63	...	14.50 ± 0.090
2009/03/26.73	917.23	91.65	...	14.41 ± 0.073
2009/04/05.79	927.29	101.71	...	15.00 ± 0.147
2009/04/10.80	932.30	106.71	...	14.94 ± 0.171
2009/04/15.80	937.30	111.72	...	14.86 ± 0.173
2009/04/20.52	942.02	116.44	...	15.23 ± 0.232

Note. [a] With reference to the explosion epoch JD 2454825.6.

Table 5
Journal of Spectroscopic Observations of SN 2008in

UT Date (yy/mm/dd/hh.hh)	JD 2454000+	Phase[a] (days)	Range (μm)	Telescope[b]	Grating (gr mm^{-1})	Slit Width ($''$)	Dispersion (Å pixel^{-1})	Exposure (s)	S/N[c] (pixel^{-1})
2008/12/31/22.80	832.45	+7	0.45–1.00	HET	300	1.0	5.0	600	45
2009/01/07/22.31	839.43	+14	0.45–1.00	HET	300	1.0	5.0	600	43
2009/02/17/19.74	880.32	+54	0.38–0.68	IGO	600	1.5	1.4	1800	34
2009/02/22/22.50	885.44	+60	0.45–1.00	HET	300	1.0	5.0	600	35
2009/03/22/20.45	913.35	+87	0.38–0.68	IGO	600	1.5	1.4	1800	38
2009/03/25/22.13	916.42	+90	0.38–0.68	IGO	600	1.5	1.4	2700	35
2009/04/03/19.14	925.26	+99	0.38–0.68	IGO	600	1.5	1.4	1800	35
2009/04/03/20.98	925.33	+99	0.60–1.00	BTA	550	2.1	3.5	3×900	60
2009/04/22/15.49	944.14	+118	0.38–0.68	IGO	600	1.5	1.4	1800	11
2009/04/23/18.00	945.25	+119	0.38–0.79	BTA	600	2.1	3.5	3×900	65
2009/05/17/02.38	968.10	+143	0.33–0.80	NTT	300	1.0	4.0	2700	59

Notes.
[a] With reference to the explosion epoch JD 2454825.6.
[b] HET: Low-Resolution Spectrograph on the 9.2 m Hobby Eberly Telescope; IGO: IFOSC on 2 m IUCAA Girawali Observatory, India; BTA: SCORPIO on the 6 m Big Telescope Alt-azimuth, Special Astrophysical Observatory, Russia; NTT: EFOSC2 on the 3.6 m New Technology Telescope, ESO, Chile.
[c] At 0.6 μm.

BTA, and NTT, the resolution near 6000 Å is about 10 Å, 14 Å, and 12 Å, respectively.

3. LIGHT-CURVE EVOLUTION

According to theoretical interpretation, the entire broadband evolution of Type II SNe can be segmented into three phases: the rising phase, the plateau phase, and the nebular phase.

3.1. The Rising Phase

The rising phase of the light curve is associated with the shock breakout phenomenon having been theoretically predicted for an SN explosion, in which the radiation-dominated shock wave, generated through the reversal of iron core-collapse, starts to propagate outward through the onion-shell-like layers of the progenitor; when the shock reaches regions with an optical depth of a few tens to unity, the radiation behind the shock escapes the outer surface giving rise to a hot ($T > 10^5$ K) fireball which emits quasi-blackbody radiation in UV and soft X-rays. This phenomenon is called shock breakout, and depending on envelope mass, density structure, and wind properties of the progenitor, the breakout light curve may last from a few hours to a few days (Grassberg et al. 1971; Chevalier 1976; Falk & Arnett 1977). Due to the short timescale, the detection of shock breakout is rare, and only recently were the UV light curves of the entire shock breakout phase lasting several hours reported for two Type IIP SNe—SNLS-04D2dc and SNLS-06D1jd (Gezari et al. 2008; Schawinski et al. 2008). Observation of the earliest UV and optical light curves of IIP SNe is crucial to model the shock breakout light curves and constrain the properties of SN
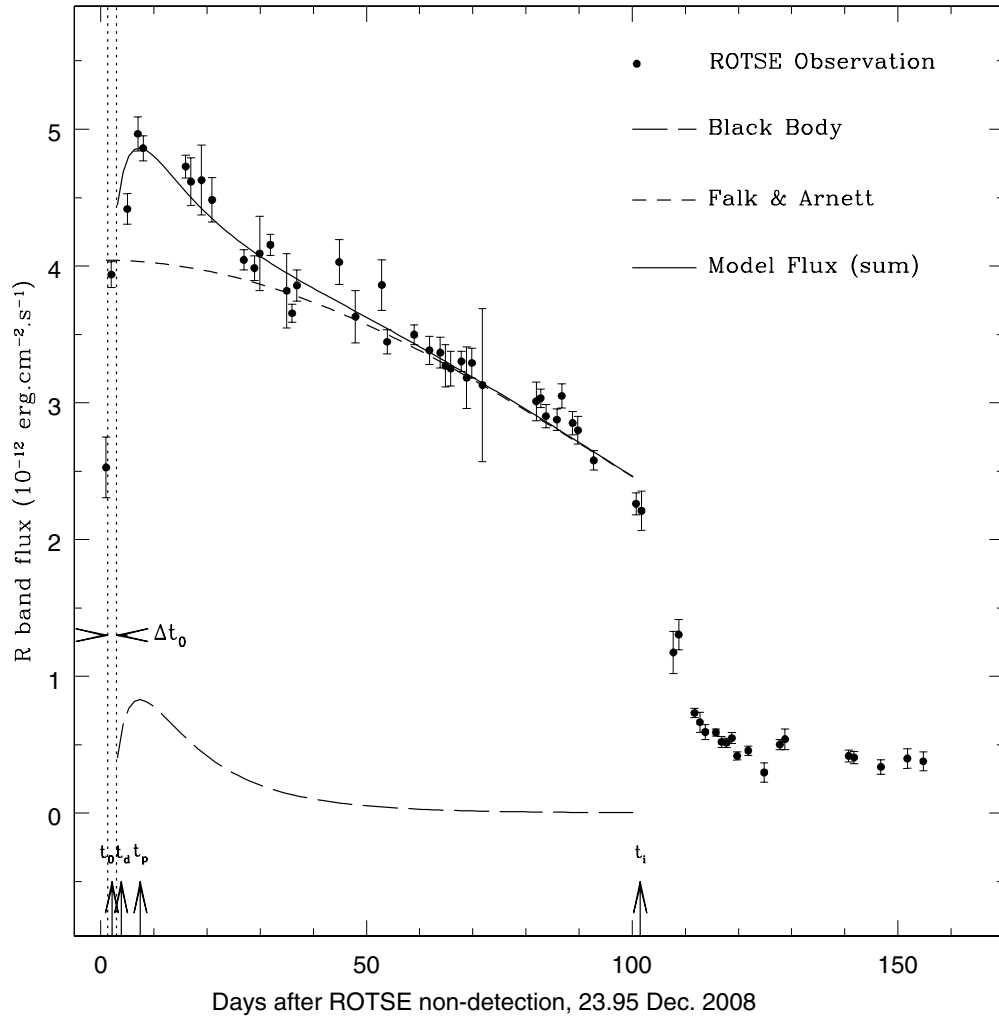
Figure 3. ROTSE R-band light curve of SN 2008in. Reference time for the x-axis is the epoch of ROTSE non-detection on 2008 December 23.95. The evolution of the post-shock breakout flux has been modeled by using the simple analytical expressions given in Cowen et al. (2010) and Arnett (1980). The best-fit time for shock breakout is marked with t_0 while Δt_0 shows the duration of uncertainty. t_d is the time of discovery reported by Nakano et al. (2008). t_p is the time when R light shows the peak. t_i is the time of inflection obtained using the procedure of Elmhamdi et al. (2003a).

progenitors (Tominaga et al. 2009). The earliest SNe IIP optical light curves have been studied in the past for SN 2005cs by Pastorello et al. (2009) and for SN 2006bp by Quimby et al. (2007) and the optical rising phase is rarely observed.

We model the early optical (ROTSE-IIIb R-band) light curves of SN 2008in using a simple model and put an observational constraint on the epoch and duration of shock breakout. Following the formulation of Waxman et al. (2007), it can be shown that just after the shock breakout, the intensity of the SN light at a fixed wavelength is proportional to the intensity of blackbody radiation at that wavelength (see Equation (1) of Cowen et al. 2010), while for the plateau phase Arnett (1980) derived an analytical expression (Equation (39) of that paper); hence by combining these two equations one can approximate the overall intensity profile of a Type II SN during the rising phase with the plateau with the following expression:

$$I_{\rm SN}(t) = \frac{A}{\exp[B \times (t - t_0)^{0.5}] - 1} \times (t - t_0)^{1.6}$$
$$+ C \times \exp[-\{(t/D) + (t/E)^2\}]. \tag{1}$$

Here, the first term represents the phase associated with the shock breakout while the second term represents the plateau

phase. Here t is the time measured in days since 2008 December 23.95 (JD = 2454823.5), the epoch when ROTSE had a non-detection of the SN with limiting magnitude 16.16 in the R band. The time of shock breakout, t_0, along with the constants A, B, C, D, and E, are free parameters of the fit. The values of these constants depend on the nature of the progenitor and the kind of explosion. The above model is fitted to the ROTSE data using the χ minimization technique (Press et al. 1992) and the fit is shown in Figure 3. We obtained a value of the shock breakout time as $t_0 = 2.13 \pm 0.83$ day. This value of t_0 is consistent with the first data point observed from ROTSE. We shall adopt t_0 corresponding to JD = 2454825.6 as the explosion epoch for all the phases of SN 2008in. It is noted that at V and R bands, the SN was detected by Nakano et al. (2008), just 2.4 days after the shock breakout. We note, however, that depending on the extent of the envelope the true core reversal marking the SN explosion would have occurred a few hours earlier (e.g., SN 1987A) or a few days earlier for a red supergiant envelope $\sim$50,000 $R_\odot$ (Quimby et al. 2007).

In Figure 3, t_p (+5.3 days) corresponds to the peak of the ROTSE R-band light curve. A similar peak in the UV light curves of the post-shock breakout phase of the Type IIP supernova SNLS-04D2dc lasting several days was identified as a secondary
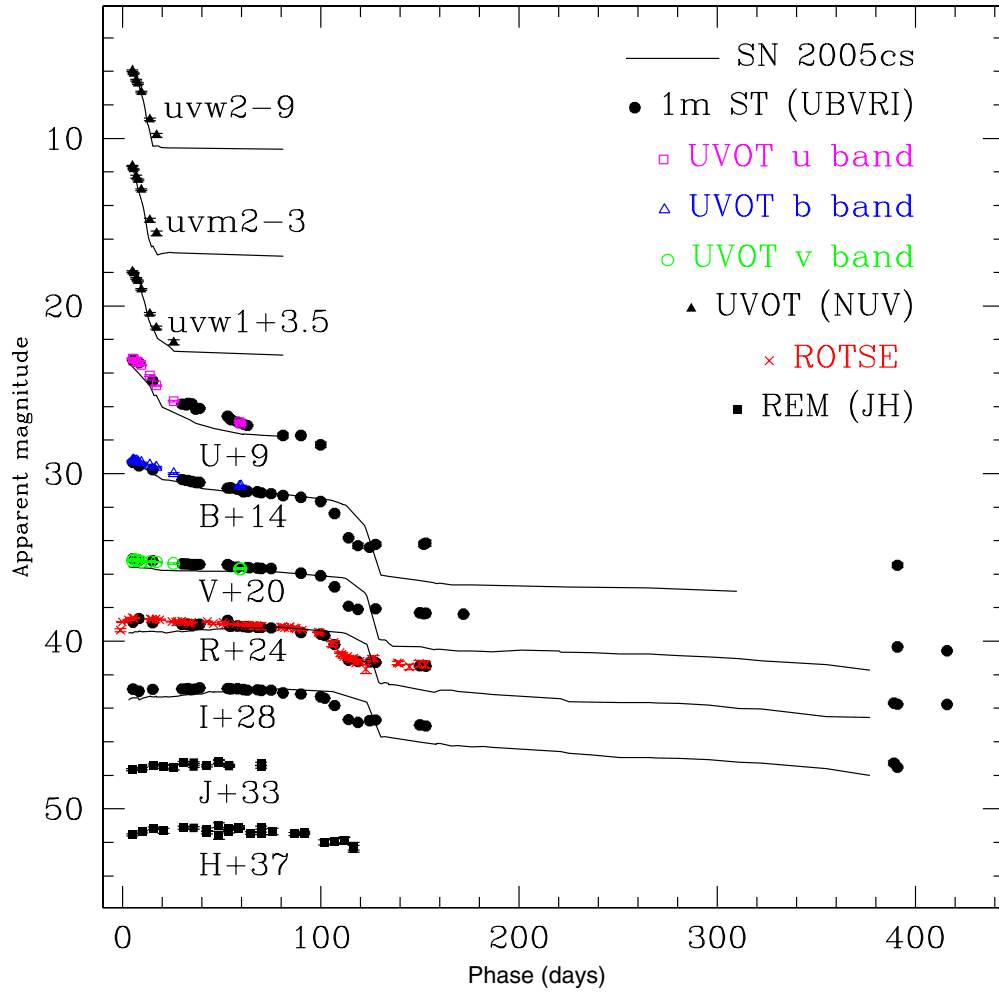
Figure 4. Light curves of SN 2008in in the UV, optical, and NIR bands. The light curves of archetypal low-luminosity SN 2005cs are overplotted for comparison (data are taken from Brown et al. 2009; Pastorello et al. 2009). The light curves of SN 2005cs are scaled in magnitude to match the light curves of SN 2008in.
(A color version of this figure is available in the online journal.)

peak and this peak was explained as the shift of the spectral energy distribution toward longer wavelengths due to the rapid fall in temperature during free adiabatic expansion of optically thick plasma led by a collisionless shock (Schawinski et al. 2008; Tominaga et al. 2009). For SN 2008in we identify the peak in the ROTSE R-band curve as a secondary peak and also speculate that for a few other type IIP SNe such as 1999em, 1999gi, and 2005cs, where very tiny peaks before the plateau light curve were observed, such features are basically the footprints of the secondary peaks which could be a consequence of shock breakout.

3.2. The Plateau and Nebular Phase

The entire UV, optical, and NIR light curves of SN 2008in are shown in Figure 4. For comparison, the light curves of the archetypal low-luminosity SN 2005cs (Brown et al. 2009; Pastorello et al. 2009) are also plotted by scaling them in magnitude to match the observed plateau of SN 2008in. In the early plateau phase, a rapid drop in the UV flux and a slowly declining or constant optical and NIR flux are clearly apparent. The $uvm2$ magnitude declined from about 14.7 to 18.7 mag within 12 days. The decline rates of the SN 2008in flux in UVOT, U, B, and V bands are almost identical with that of SN 2005cs. Starting from the $uvw2$ until the R band, the measured decline rates from shock breakout to the plateau

phase are approximately 0.32, 0.34, 0.25, 0.13, 0.04, 0.01, and 0.01 mag day^{-1}. The IJH light curves are almost flat even at early phases of the plateau. For this SN, the plateau is well sampled in the $BVRI$ bands, so we can accurately determine the plateau duration. As discussed in Section 3.1, the secondary peak ($t_p \sim$ +5.3 days) in the prompt light curve is generated by the gradually cooling shock-heated SN atmosphere and after that the plateau mechanism starts to dominate. On the other hand, between the plateau and the nebular phase there is another transitional state, when an inflection in the light curve can be seen (Section 7.1). Hence, the plateau duration is precisely the time span between the secondary peak and the inflection. The inflection (t_i) in the V-band light curve is observed to occur nearly 103.2 days after the shock breakout. Hence, the time interval between t_i and t_p is assumed as the duration of the plateau, i.e., (103.2 − 5.3) ∼ 98 days.

Once the hydrogen envelope is fully recombined and the ejecta becomes optically thin, the light curve enters the nebular phase and it is sustained mainly by the energy output from radioactive decays of the iron-group elements. During the plateau to nebular transition phase, the V-band magnitude drops from ∼16.0 mag at around +90 days (still in the plateau) to 18.1 mag at +122 days (in the exponential light-curve tail), i.e., ∼2 mag in about one month. This drop is remarkably smaller than that of SN 2005cs, but consistent with the 2–3 mag drop
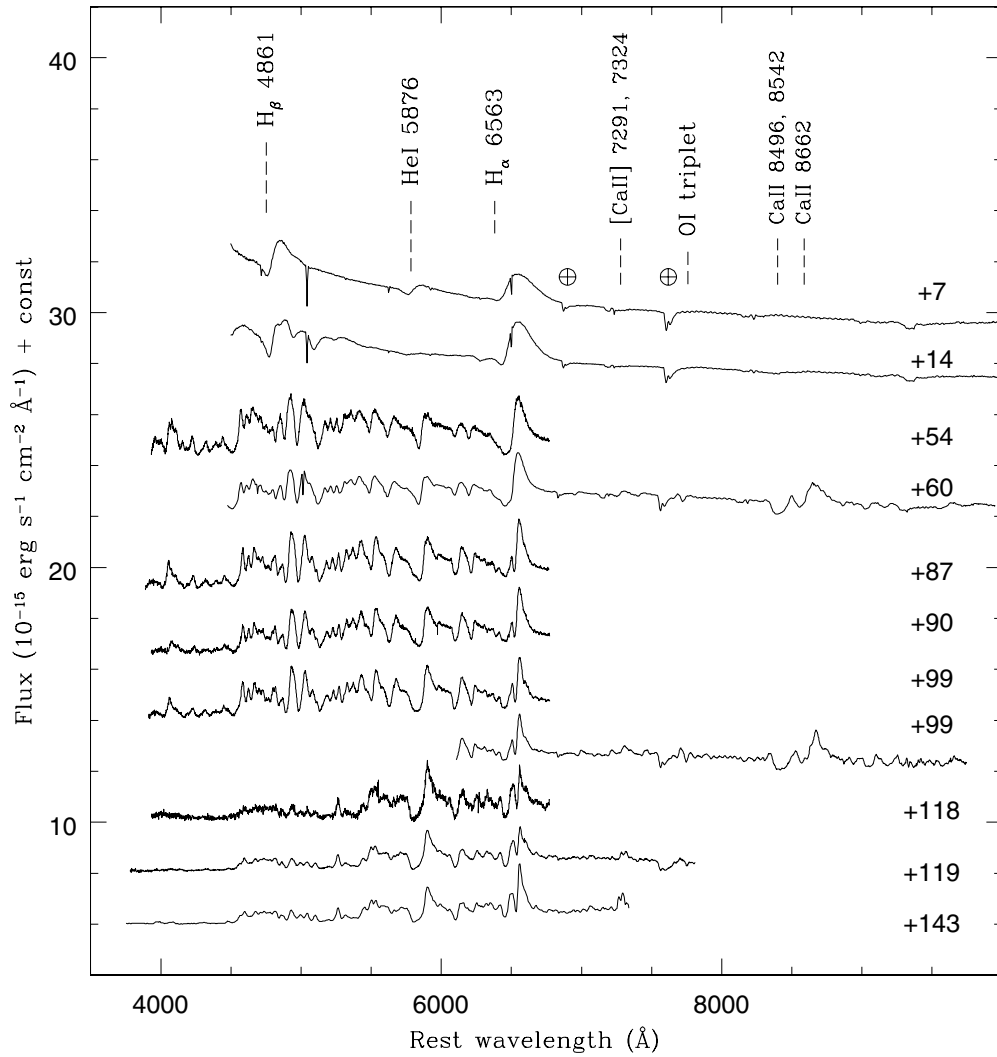
Figure 5. Doppler-corrected flux spectra of SN 2008in observed from +7 days to +143 days. Prominent lines are marked. Telluric features are marked with the ⊕ symbol. The sharp absorption dips seen near 5000 Å and 6500 Å in the +7 day and +14 day spectra are artifacts. The spectra signify the early photospheric phase (+7 days, +14 days), the mid-plateau phase (+54 days, +60 days), the late-plateau phase (+87 days, +90 days, and +99 days), and the nebular phase (+118 days, +119 days, and +143 days).

observed in normal Type IIP SNe (Olivares et al. 2010). A linear fit to the tail from +120 days to +400 days gives the following decline rates (in mag $(100\,\text{days})^{-1}$): $\gamma_B \sim 0.44$, $\gamma_V \sim 0.84$, $\gamma_R \sim 0.91$, $\gamma_I \sim 1.03$ at B, V, R, and I bands, which are similar to the values found in normal IIP SNe and comparable with the decay slope of ^{56}Co to ^{56}Fe, i.e., $0.98\,\text{mag}\,(100\,\text{days})^{-1}$.

4. SPECTROSCOPIC EVOLUTION

The spectra of SN 2008in at 10 phases from +7 days to +143 days are shown in Figure 5. The spectra are corrected for the recessional velocity of the host galaxy ($\sim$1567 $\pm$ 3 km s^{-1}).[23] Spectral features are mainly identified as per previously published line identifications for IIP SNe (Leonard et al. 2002; Pastorello et al. 2004). The two earliest spectra (+7 days and +14 days) show the blue continuum of blackbody emission and have broad P-Cygni profiles of Hα, Hβ, and He I λ5876. The next two spectra (+54 days and +60 days) represent the mid-plateau phase and are marked by a decrease in the continuum and the appearance of more P-Cygni profiles

for the permitted metallic (Fe II, Sc II, Ti II, Ba II, and Mg II), O I λ7773, Na I D, and Ca II IR triplet lines similar to other normal Type IIP SNe (see Roy et al. 2011 and references therein). The spectra at phases +87 days, +90 days, and +99 days represent the end stages of the plateau and these are marked by a redder continuum and decreasing line widths of hydrogen lines. The +118 day, +119 day, and +143 day spectra represent the nebular phase having negligible continuum and are marked by pronounced emissions of forbidden lines [Ca II] $\lambda\lambda$7291, 7323, and fading of the absorption features of hydrogen and metallic lines.

In Figure 6, we compare the +99 day spectrum of SN 2008in with the spectra of other Type IIP SNe observed at similar phases that is at roughly the time when the light curve changes from the photospheric plateau to the nebular phase. The phases quoted for each event are with reference to the moment of inflection (t_i; see Figure 3). The narrow P-Cygni Hα profile and the presence of strong lines of Ba II at λ6142 and λ6497 of SN 2008in show striking resemblance to the low-luminosity SNe 1997D, 1999br, 1999eu, 2001dc, and 2005cs. On the other hand, the normal Type IIP SNe 2004et and 2008gz show broader profiles of Hα and weaker lines of Ba II. It is noted that in the blue wing of Hα
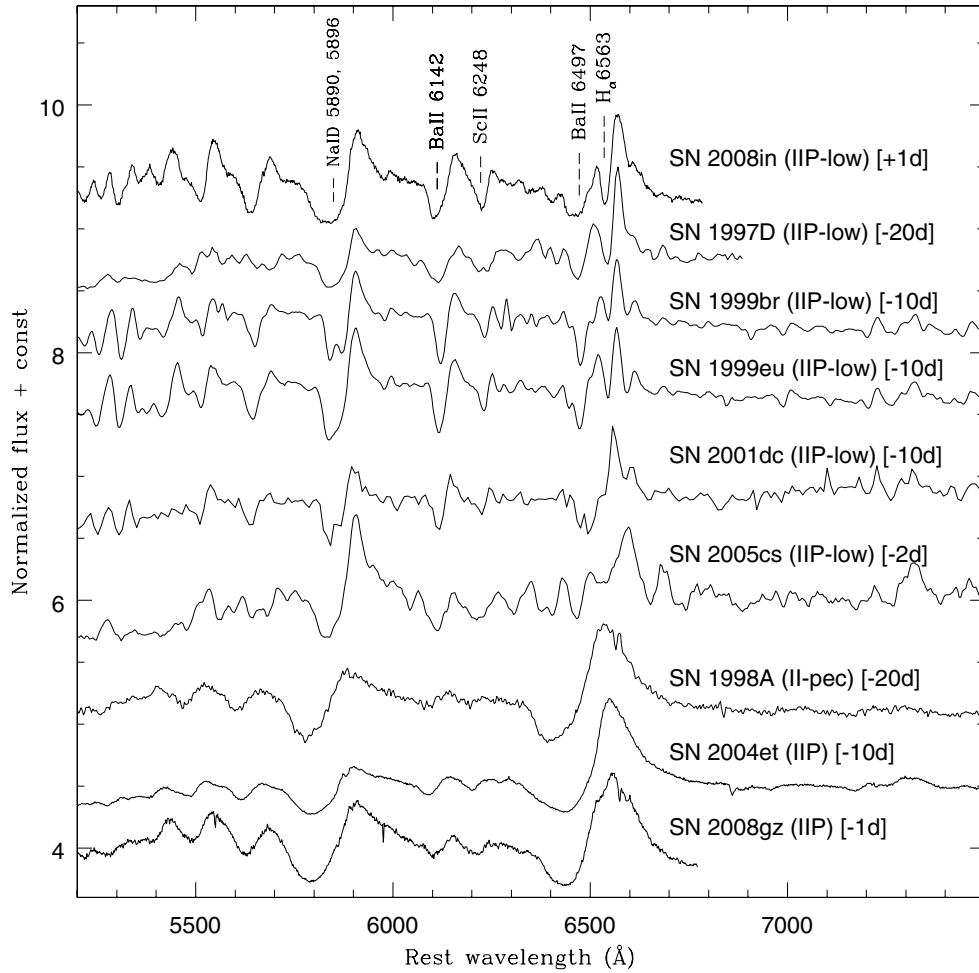
Figure 6. End plateau spectrum (+99 days) of SN 2008in is compared with five low-luminosity SNe 1997D, 1999br, 1999eu, 2001dc, and 2005cs (Pastorello et al. 2009 and references therein), two normal SNe 2004et (Misra et al. 2007) and 2008gz (Roy et al. 2011), and a peculiar Type II SN 1998A (Pastorello et al. 2005), observed at comparable epochs. The phases quoted for each event are with reference to the moment of inflection (t_i; see Figure 3), which marks the highest rate of decline in the V-band light curve during the end of the plateau and the beginning of the nebular phase (Elmhamdi et al. 2003a). All the spectra have low spectral resolution (∼10 Å). The P-Cygni features of Na I D, Ba II λ6142, Sc II λ6248, Ba II λ6497, and Hα are marked.

more metallic lines get resolved than in the normal IIP SNe and this arises due to smaller line widths of hydrogen lines seen in low-luminosity IIP SNe (Fraser et al. 2010 and references therein). In addition, the Ba II line in the low-luminosity SNe shows stronger absorption components due to lower ejecta temperature than that in the normal luminosity Type IIP SNe 2004et and 2008gz (Turatto et al. 1998). In Figure 7, we have identified the spectral features in a late-plateau phase (+99 days) spectrum which covers the full wavelength range from 0.4 to 0.95 μm. For line identification we have followed Pastorello et al. (2004), where different spectral lines were identified for the +102 day spectrum of a low-luminosity SN 1999br. We are able to identify all the features and the spectral profiles of all the elements are similar to the archetypal low-luminosity IIP SNe 1997D, 2005cs, and 1999br (Pastorello et al. 2004 and references therein).

Figure 8 shows the spectral evolution of Hα, Hβ, Na I D, Fe II, Ba II, and Sc II lines. In Figure 9 (left panel), we show the expansion velocities of the ejecta derived from Balmer and Fe II lines. The latter is a good indicator of photospheric velocity. The expansion velocities of the H-envelope are estimated using absorption minima of the P-Cygni profiles and at the two earliest phases (+7 days and +14 days) Hα and Hβ show a broad P-Cygni profile which, with time, becomes narrower at later

phases keeping the position of the emission peak centered near zero velocity. The Hα line velocity starts at about 7000 km s^{-1} at +10 days, reaches 4000 km s^{-1} at +50 days, and flattens at a level of 1200 km s^{-1} in the nebular phases. It can be seen from the right panel of Figure 9 that in the comparable phases the Hα line velocities of low-luminosity SNe are less than half those of normal IIP SNe 1999em and 2004et, whereas the SN 2008in velocities are more like low-luminosity SN 2005cs. To estimate the photospheric velocity of the transient, we have computed the velocities of different Fe II lines λ4924, λ5018, and λ5169 at different phases. The first marginal detection of these lines is in the +14 day spectrum and they became prominent in later stages of evolution. For SN 2008in, the average velocity of these lines (and hence roughly the photospheric velocity) at +14 days is about 4450 km s^{-1}, which is comparable with that of low-luminosity SNe and much less than ordinary Type IIP events (see Figure 12 of Pastorello et al. 2009).

The emergence of absorption dips in the blue wings of Hα is clearly seen in the post +60 day spectra[24] and the absorption dips have been marked with A, B, and C in Figure 8. We distinguish "A" as an absorption dip due to Ti II and Hα and

---

[24] This is the first time that the rapidly changing evolution of Hα profiles during the late plateau to nebular phase has been so densely covered in a low-luminosity SN.
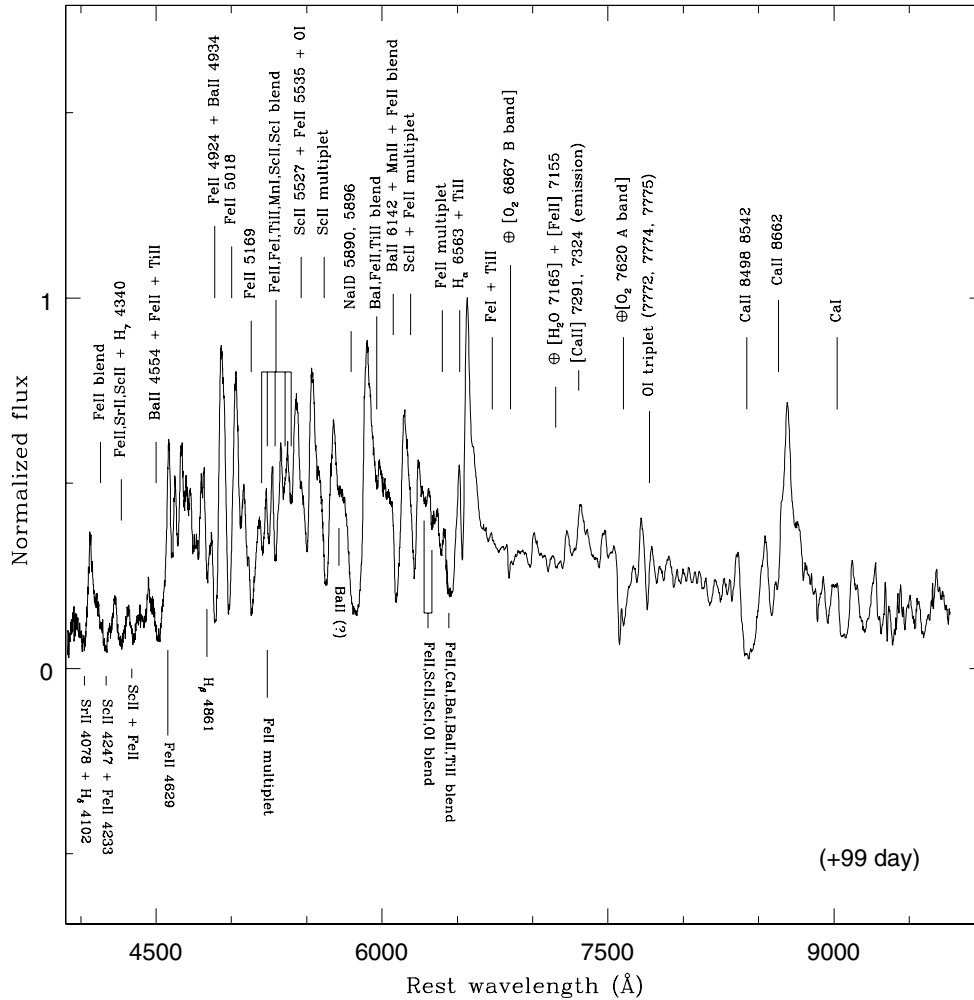
Figure 7. Spectral line identifications in a late-plateau phase (+99 days) spectrum are shown. Spectral features are mainly identified as per previously published line identifications for IIP SNe (Leonard et al. 2002; Pastorello et al. 2004). Telluric features are marked with the "⊕" symbol.

its equivalent width (EW) increases from 12.85 Å at +60 days to 19.45 Å at +143 days. This progressively stronger absorption dip requires a steep deceleration of the Hα emitting zone along with its depletion by inner metal shells (like Ti II). The broader absorption dip "B" is identified as a blend of Ba II λ6497, Ba I, Ca I, and Ti II. An exceptionally strong Ba II line is quite typical for cooler ejecta of less energetic faint SNe. The segment "C" is speculated to be a footprint of Fe II multiplets as the evolution of its linewidths seems to be correlated with the other Fe II lines. It is noted, however, that in a few normal Type IIP SNe 1999em, 2004et, and 2008gz, the spectral feature near "C" at early plateau phases was also identified as a signature of a high-velocity Hα component, and in the present spectra its presence cannot be completely ruled out.

The evolution of Hβ is similar to the evolution of Hα. The P-Cygni profile of Hβ is clearly visible in the +7 day spectrum, and later on, the emission component is blanketed by various metal lines, mainly due to Fe II λ4924, λ5018, and λ5169. Traces of Hβ and Fe II absorption dips indicate that from the beginning of the nebular phase H shells of ejecta and the regions containing Fe II ions move with a comparable velocity, reaching an asymptotic value of ∼1000 km s^{-1} nearly 140 days after the explosion. In the +14 day spectrum, Fe II lines are marginally detected while in the spectra between +60 days and +99 days they are prominent. We investigated the temporal change of EW of a relatively less blended Fe II λ4924; from the spectra

normalized to the Hα peak value we found an EW ∼ 0.67 Å at +14 days, increasing to 17.45 Å at +54 days and to 26.53 Å in the +99 day spectrum. Later on, the EW decreased to 19.07 Å in the +118 day spectrum and finally reached 18.27 Å in the +143 day spectrum. This rapid fall in the EW of inner metal-rich shells plausibly indicates a decrease in the opacity of the SN inner ejecta.

Traces of the He I λ5876 line are also seen in the +7 day spectrum (Figure 8). The ratio of EWs between Hα and He I for this spectrum is EW(Hα)/EW(He I) ∼ 1.99. In the +14 day spectrum, this ratio has increased to 5.36. The steep decrement in EW of He I seems to be due to a quick recombination of He I ions as a result of the rapid fall in temperature of the constantly rarefying ejecta. From +54 days, the emerging P-Cygni feature of Na I D becomes prominent. This feature seems to be a perfect P-Cygni throughout our entire spectral sequence. It simply indicates a uniform spherical distribution of Na I in the SN ejecta. In the three high S/N spectra labeled with +54 days, +60 days, and +87 days, a tiny absorption dip overlaid on the emission component of the Na I D P-Cygni is seen, and since these spectra are redshift corrected, these dips are impressions of intervening interstellar matter present in the host galaxy. The absence of any similar absorption dip in the blue wing of the Na I D profile, expected from Galactic interstellar matter, confirms that there is little absorption from the Milky Way in the line of sight of SN 2008in.
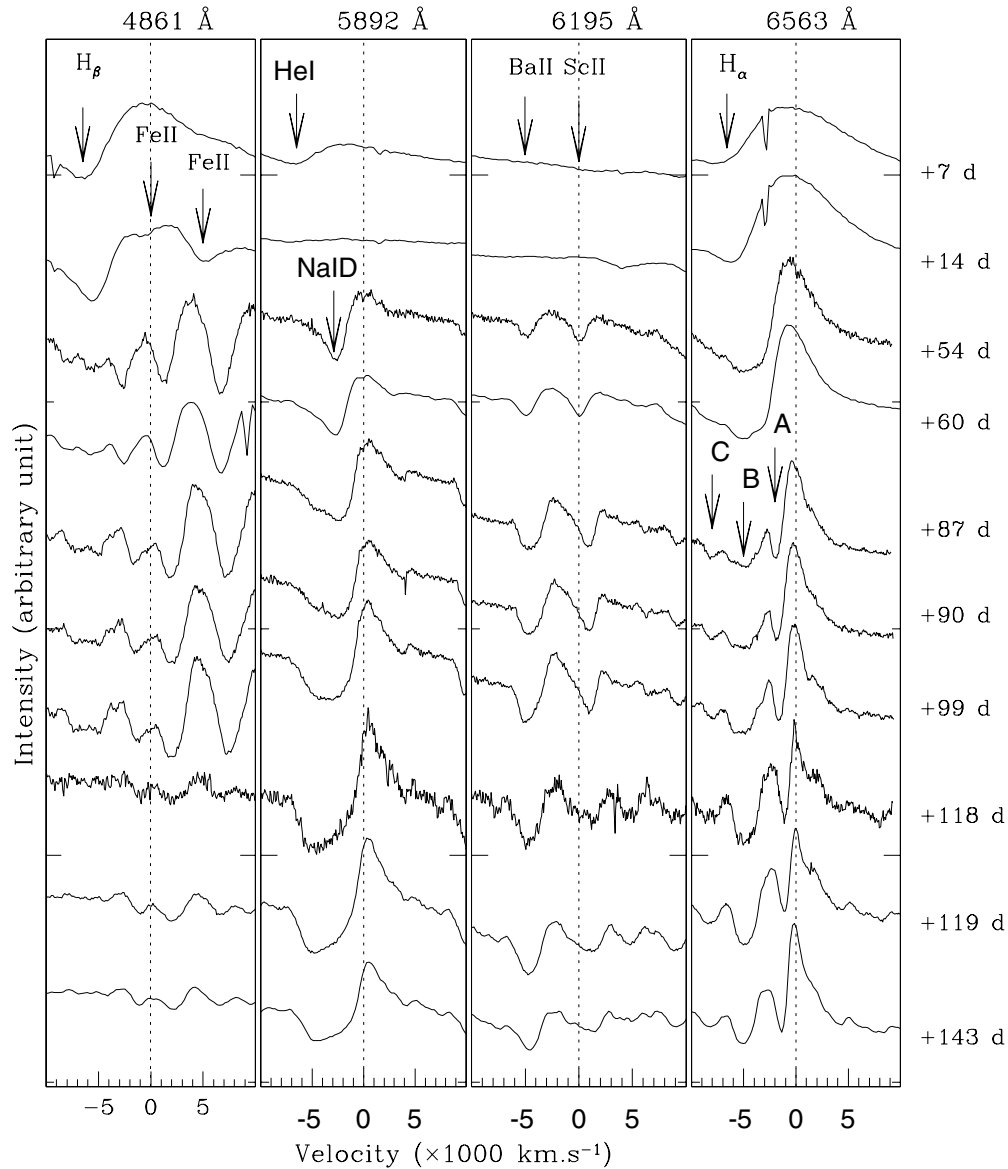
Figure 8. Spectral evolution of Hβ, Fe II λ4924, Fe II λ5018, He I λ5876, Na I D λλ5890, 5896, Ba II λ6148, Sc II λ6248, Ba II λ6497, and Hα lines of SN 2008in during its transition from the plateau to the nebular phase. The dotted line at zero velocity corresponds to the rest wavelength, marked at the top of each panel. The sharp absorption dips seen in the Hα profile for +7 day and +14 day spectra are artifacts.

The spectral evolution of Sc II λ6248 and the s-process element Ba II λ6142 is clearly seen in SN 2008in. In the +7 day and +14 day spectra, there is no clear evidence for the presence of these two elements; however, in the +54 day spectrum they are prominent. The absorption components become stronger with time and persist until the +143 day spectrum. In contrast, in the normal Type IIP SNe 2004et (Sahu et al. 2006), 1999em (Elmhamdi et al. 2003b), and 2008gz (Roy et al. 2011) these features disappeared at ∼170 days after the explosion. The ejecta of underluminous Type IIP SNe expand at a lower velocity than those of normal ones. So, the Ba lines in low-luminosity events persist for a longer time just because the ejecta takes more time to cool down. As a result, it takes longer to become optically thin.

In the nebular phase, the forbidden lines [Ca II] λλ7291, 7323, [O I] λλ6300, 6364, and [Fe II] λ7155 are among the strongest features visible in the spectra. Also, the line ratios of emission lines of Ca II and the O I doublet in late nebular phases are a good indicator of the progenitor mass (Fransson & Chevalier

1987). In Figure 10, we compare the +139 day and +283 day spectra of SN 19997D (Benetti et al. 2001) with the nebular phase spectra of SN 2008in. The [Ca II] doublet is seen in the +99 day, +119 day, and +143 day spectra of SN 2008in, whereas a small footprint of the O I doublet can be seen in the +143 day spectrum. The [Fe II] line is not seen in our spectra. Considering that the explosion epoch of SN 1997D was quite uncertain, it is likely that the spectral evolution of Hα and forbidden lines of SN 2008in is quite similar to that of SN 1997D.

5. EXTINCTION AND DISTANCE TOWARD SN 2008in

In order to determine the bolometric light curve and other physical parameters, a correct estimate of the extinction and distance toward the SN is essential. We adopt the Galactic reddening along the line of sight of SN 2008in as derived from the 100 μm all sky dust extinction map (Schlegel et al. 1998), i.e., $E(B - V) = 0.0224 \pm 0.0003$ mag. In order to estimate reddening due to the host galaxy M61, we used the
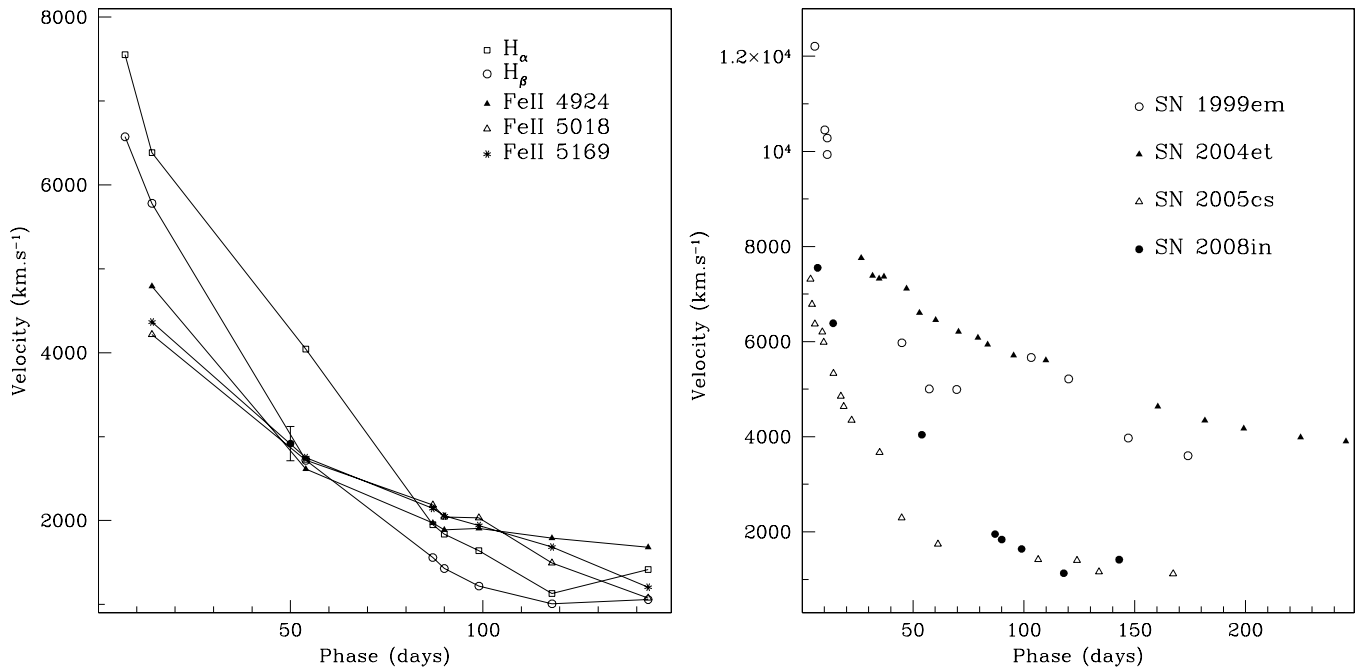
Figure 9. Evolution of the expansion velocity of SN 2008in. The left panel shows the velocity of different elements in the ejecta of SN 2008in. The black filled circle shows the estimated value of mid-plateau photospheric velocity, calculated using the relation mentioned in Roy et al. (2011). The right panel shows a comparison of velocity derived from Hα with that of a low-luminosity event like SN 2005cs (Pastorello et al. 2009) and normal Type IIP SNe 1999em (Elmhamdi et al. 2003b) and 2004et (Sahu et al. 2006).

spectrum of SN 2008in taken on 2009 February 17 from the 2 m IGO telescope having good S/N (∼40) and corrected for mean heliocentric radial velocity of the host ($cz \approx 1567 \pm 3\,\mathrm{km\,s^{-1}}$). Near the zero velocity, the spectrum showed a tiny absorption feature overlaid on the emission component of the P-Cygni profile of Na I D (Section 4). The EW of this absorption feature was computed as 0.535 ± 0.713 Å. The error in EW is estimated using Equation (6) of Vollmann & Eversberg (2006). It is known that the EW of the interstellar absorption bands is well correlated with the reddening $E(B-V)$ estimated from the tail of the SN Ia color curve (Barbon et al. 1990; Richmond et al. 1994; Turatto et al. 2003), and hence using the empirical relation $E(B-V) = -0.01 + 0.16\mathrm{EW}$ (EW in Å), given by Turatto et al. (2003), we obtain the host contribution as $E(B-V) \approx 0.076 \pm 0.104$, which is considerably higher than the Galactic contribution. This is consistent with the absence of any absorption feature due to Galactic interstellar matter in the blue wing of the emission component of the Na I D profile. Consequently, we adopt an $E(B-V)$ (estimated as a sum of Galactic and host galaxy reddening) of 0.0984 ± 0.104 mag for SN 2008in. This corresponds to a visual extinction (A_V) of 0.305 ± 0.322. Considering the uncertainty in the $E(B-V)$ estimated using Na I D lines, a lower value of $E(B-V)$ of 0.0448 ± 0.0006 mag (twice the Galactic reddening) and the corresponding A_V of 0.139 ± 0.002 cannot be ruled out. We will discuss its implication for the derived properties of the SN.

The Hubble flow distance of the host galaxy M61, after correction for the Virgo infall, is estimated as 13.7 ± 1.1 Mpc.[25] The distance estimated through the Tully–Fisher method is 12.1 ± 2.7 Mpc.[26] Additionally, we also calculated the distance following the Standard Candle Method for Type II SNe

(Hamuy & Pinto 2002; Hamuy 2005; Hendry et al. 2005). It is found that there is a strong correlation between the distance of Type IIP SNe along with their mid-plateau apparent V- and I-band magnitudes and the mid-plateau photospheric velocity, for a given cosmological model. For SN 2008in we estimate the mid-plateau (∼+50 days) apparent magnitudes ∼15.56 ± 0.05 mag for V and ∼14.77 ± 0.06 mag for the I band. Considering the V- and I-band extinctions toward the SN, 0.305 ± 0.322 mag and 0.183 ± 0.193 mag, respectively, we derive a distance of ∼12.23 ± 1.87 Mpc. The adopted value of mid-plateau photospheric velocity is $2694.67 \pm 70\,\mathrm{km\,s^{-1}}$ (see Section 7.2). Combining the above three measurements, we adopt the weighted mean distance of 13.19 ± 1.09 Mpc, which corresponds to a distance modulus of 30.6 ± 0.2.

6. COLOR EVOLUTION AND BOLOMETRIC FLUX

Figure 11 shows the temporal evolution of the reddening-corrected broadband colors of SN 2008in. For comparison, we overplot the color curves for well-studied SNe 1987A (Suntzeff & Bouchet 1990), 1999em (Elmhamdi et al. 2003b), 2004et (Sahu et al. 2006; Maguire et al. 2010), 2005cs (Pastorello et al. 2009), and SN 2008gz (Roy et al. 2011). After small differences during the initial phases, the plateau phase color evolution of all Type II SNe is more or less similar. The $(U-B)_0$ and $(B-V)_0$ colors are blue during early photospheric phases and they become redder by about 1–2 mag in the plateau phase while the $(V-R)_0$ and $(V-I)_0$ colors evolve slowly and become red only by about 0.5 mag. The $(J-H)_0$ color remains constant at ∼0.25 mag. During the transition phase from plateau to nebular, the low-luminosity SN 2005cs showed a striking red peak in the $(B-V)_0$, $(V-R)_0$, and $(V-I)_0$ colors. For SN 2008in, this red peak is not present and its color evolution is found to be consistent with the normal Type IIP SNe.

The quasi-bolometric light curve estimated from the UV, optical, and IR broadband (*UVOIR*) magnitudes of SN 2008in

---
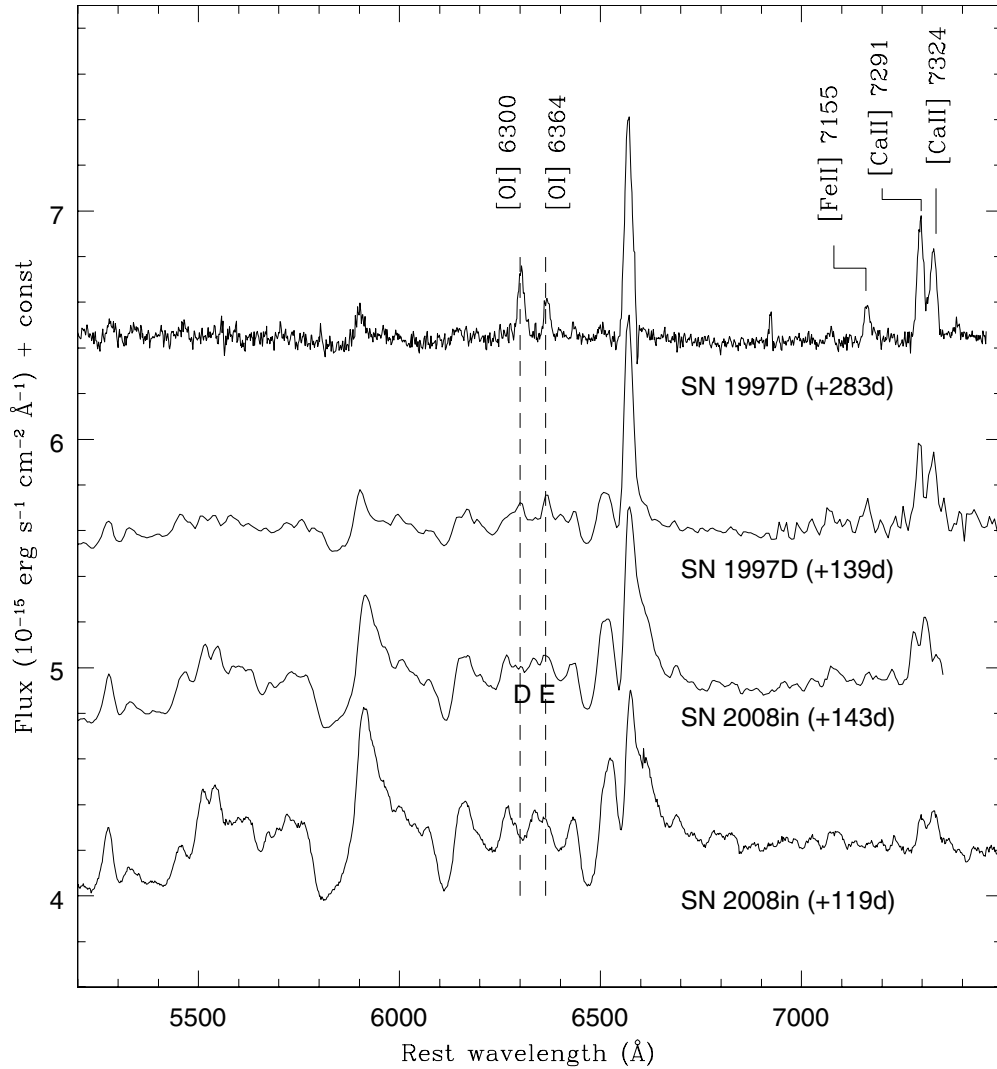
Figure 10. Forbidden lines during the nebular phases of SN 2008in are compared with the low-luminosity SN 1997D. The lines [O I], [Fe II], and [Ca II] are marked.

is shown in Figure 12 along with those of other Type II SNe. The extinction-corrected magnitudes are first converted into fluxes using zero points given by Bessell et al. (1998) and then the total flux in the *UVOIR* bands is obtained after a linear interpolation and integration between 0.203 and 1.67 μm. The fluxes were calculated on those nights for which we had complete observations in *UBVRI* bands. For the initial two weeks the SN was detected by *Swift*/UVOT in near-ultraviolet bands with a significant flux density. This contribution has been accounted for while measuring the net *UVOIR* flux. It has been assumed that contribution in the *U* band is mainly important during the plateau and decreases rapidly to about 5% in the nebular phase (see Misra et al. 2007; Roy et al. 2011 and references therein). From the light curve it is noticeable that the near-ultraviolet flux is almost negligible beyond 20 days after explosion. The *JH* contribution during the plateau is calculated from our data, whereas for the nebular phase, due to lack of data, we are not able to make any direct measurement. For most low-luminosity SNe IIP, the NIR flux contribution in the nebular phase is about 50% of the total flux (Pastorello et al. 2009). We have therefore increased the net flux by 55% to account for the maximal contributions from the *U* and NIR bands at phases later than +140 days. Figure 6 and 12 clearly demonstrate that spectroscopically SN 2008in appears to be like low-luminosity

SNe IIP, but photometrically it appears quite normal. In the following section, the *UVOIR* curve is used to estimate the amount of radioactive ^{56}Ni and other physical parameters that characterize the explosion and the progenitor star.

7. PHYSICAL PARAMETERS

The physical entities that seem to govern the entire scenario are mainly associated with the nature of the progenitor and the radioactive elements (mainly ^{56}Ni) generated inside the inner portion of the ejecta during the explosion. ^{56}Ni is synthesized by the explosive burning of Si and O during the shock break-out (Arnett 1980, 1996). Over time this material is eventually converted to ^{56}Co and then to ^{56}Fe by means of radioactive transitions having decay times of 8.77 and 111.3 days, respectively. The γ-rays and neutrinos emitted during this process sustain the nebular phase light curve, and consequently the observed tail luminosity becomes a good tracer for the ejected synthesized ^{56}Ni.

7.1. Produced Radioactive Nickel

We use different methods to estimate mass of ^{56}Ni. Hamuy (2003) proposed a relation between bolometric tail luminosity and the synthesized ^{56}Ni during core-collapse SNe by
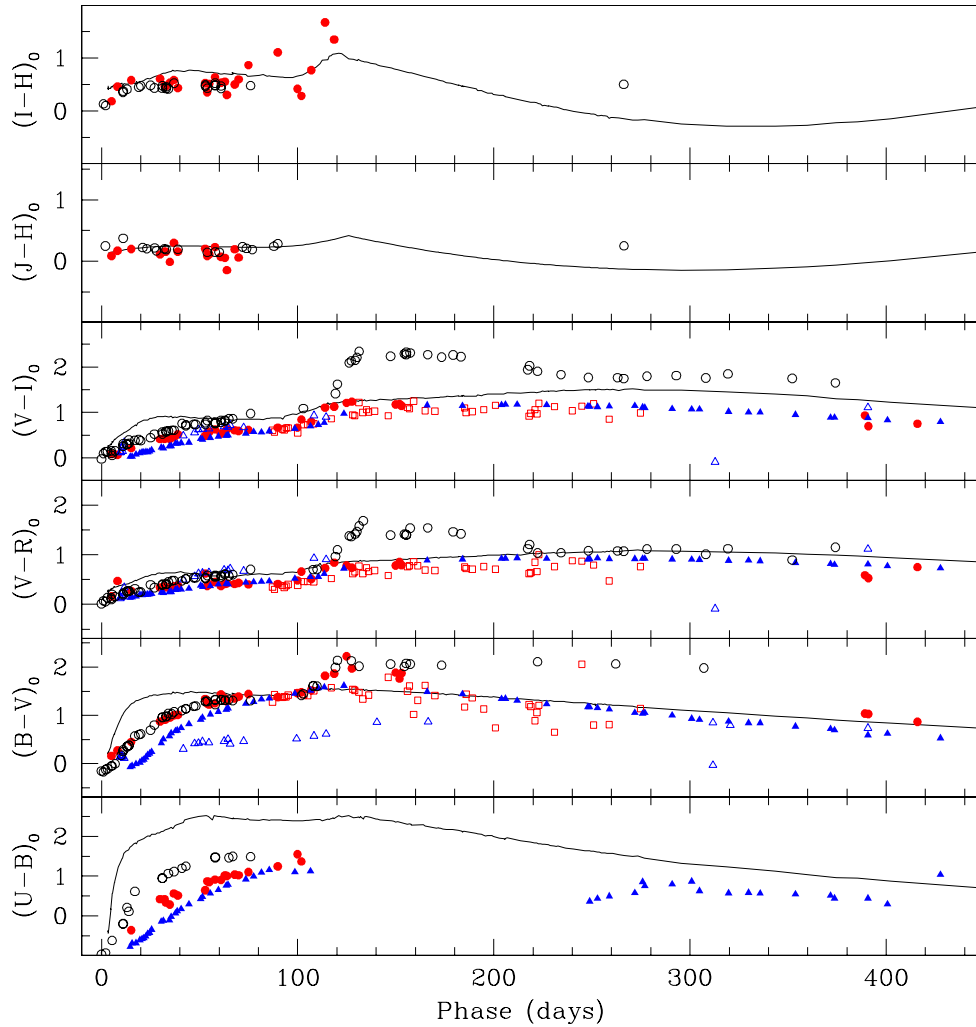
Figure 11. Color curve of SN 2008in is shown with filled circles. Also shown are the SNe 1987A (solid line), 1999em (open triangle), 2004et (filled triangle), 2005cs (open circle), and 2008gz (open square).

(A color version of this figure is available in the online journal.)

considering the underlying assumption that all γ-rays emitted during the radioactive decay make the ejecta thermalized. For SN 2008in, the time interval spanned by the observations is about 416 days, where the first $\sim$100 days are reserved for photospheric evolutionary processes. The average V band magnitude during the nebular phase calculated using the data between +114 days and +416 days is $\sim$18.91, which corresponds to the V magnitude at $\sim$ +222 days. Taking the extinction correction as $A_V = 0.305 \pm 0.322$ mag (Section 5), a bolometric correction of 0.26 ± 0.06 mag (Hamuy 2001), and a distance modulus 30.6 ± 0.2, the derived tail luminosity at this fiducial time is $(3.02 \pm 1.95) \times 10^{40}$ erg s^{-1}. Within the errors, this value is consistent with the bolometric flux at a comparable epoch, determined in Section 6. This implies that the amount of ^{56}Ni produced in this process is $M_{Ni} = 0.0157 \pm 0.0102 \, M_\odot$.

All Type IIP SNe show an inflection in the light curve during the transition from the plateau to the nebular phase. Statistically it has been shown that the steepness of the V-band light-curve slope (defined as $S = dm_V/dt$) at the inflection time (t_i) is anti-correlated with ^{56}Ni mass (Elmhamdi et al. 2003a). For SN 2008in, the V-band light curve with its well-sampled transition phase shows a value of steepness $S = 0.151 \pm 0.044$ mag day^{-1} (Figure 13) and the epoch of inflection is $t_i \approx +101.5$ days with respect to the date of discovery. This corresponds to

$M_{Ni} = 0.0175 \pm 0.002 \, M_\odot$. This result is consistent with the value measured using the Hamuy (2003) scheme. According to Elmhamdi et al. (2003a), the amount of ^{56}Ni can also be derived from the plateau absolute V-band magnitude using the relation $\log M_{Ni} = -0.438 M_V(t_i - 35) - 8.46$. Here $M_V(t_i - 35)$ is the absolute V magnitude 35 days prior to the day of inflection. For SN 2008in, $M_V(t_i - 35) \approx -15.23$, which again corresponds to a ^{56}Ni mass around $0.016 \, M_\odot$.

Comparison of the tail luminosity with that of SN 1987A—a well-studied proximate event—is also used for estimation of the ^{56}Ni mass. A linear least-squares fit on the nebular light-curve tail shows that at +222 days the luminosity of SN 2008in is about 1.54×10^{40} erg s^{-1}, while SN 1987A had a luminosity $\sim 1.10 \times 10^{41}$ erg s^{-1} (Figure 12). Since the ^{56}Ni mass produced by SN 1987A is about $0.075 \, M_\odot$, the amount of ^{56}Ni in the case of SN 2008in is $[(1.54/1.10) \times 10^{-1}] \times 0.075 \approx 0.0105 \, M_\odot$.

The above estimates are consistent with each other and hence we adopt a mean value for ^{56}Ni mass of $0.015 \pm 0.003 \, M_\odot$.

7.2. Explosion Energy and Mass of Progenitor Star

We use the radiation-hydrodynamical simulations of core-collapse IIP SNe by Dessart et al. (2010) to infer the explosion energy (E_0: kinetic plus thermal, expressed hereafter in units of 10^{51} erg, or foe). These simulations suggest that in a given

15
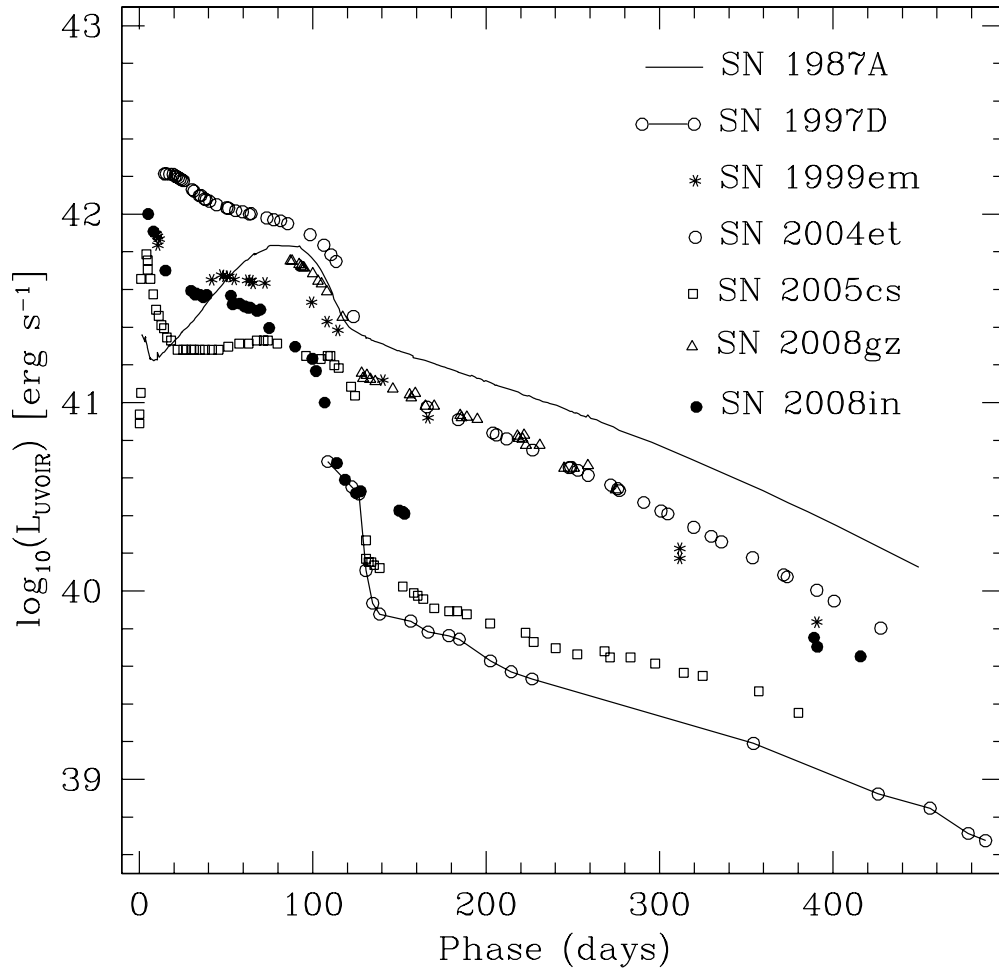
Figure 12. Comparison of the quasi-bolometric light curve of SN 2008in with the low-luminosity SNe 1997D, 2005cs; the normal SNe 1999em, 2004et, and 2008gz; and the peculiar Type II SN 1987A.

progenitor larger explosion energies yield larger ejecta velocities and this implies that the ejecta kinematics can be used to put a constraint on E_0. For SN 2008in, the expansion rate of the H-rich progenitor envelope as derived from absorption minima in Hα at 15 days after shock breakout is about $6300 \, \mathrm{km \, s^{-1}}$ (see Figure 8), which is higher than $4700 \, \mathrm{km \, s^{-1}}$ (for SN 2005cs; Pastorello et al. 2009) and lower than $8800 \, \mathrm{km \, s^{-1}}$ (for SN 1999em; Elmhamdi et al. 2003b). For the SNe 2005cs and 1999em, the simulation results (for explosion of non-rotating solar metallicity pre-SN stars) predicted $E_0 \sim 0.3$ foe and $\gtrsim 1$ foe respectively and these values are found to be consistent with that determined from the actual hydrodynamical modeling of the SN light curves, e.g., 0.4 foe (Utrobin & Chugai 2008) and 0.3 foe (Pastorello et al. 2009) for SN 2005cs; 1.3 foe (Utrobin 2007) and 1.25 foe (Bersten et al. 2011) for SN 1999em. For SN 2008in, the simulations suggest $E_0 \sim 0.5$ foe.

Accurate determinations of explosion parameters such as E_0, the ejected mass (M_{ej}), and the pre-SN radius (R_0) of the progenitor require detailed hydrodynamical modeling of the light curves and spectra and this, being a non-trivial task (beyond the scope of this paper), has only been attempted for a few SNe. In order to have an estimate of explosion parameters of SN 2008in here, we employ the analytical relations derived by Litvinova & Nadezhin (1985) correlating the observed parameters (M_{Vmp}: the mid-plateau absolute magnitude at V; v_{mp}: the mid-plateau photospheric velocity; and Δt_p: the

plateau duration) with the physical parameters (E_0, M_{ej}, and R_0) based on a grid of hydrodynamical models for different values of physical parameters for Type IIP SNe. We note, however, that these approximate formulae have limitations owing to the poorly measured observables and the simplified physical conditions such as non-inclusion of the effect of nickel heating, use of old opacity tables, neglecting the effect of line opacity, and using outdated pre-SN models (Smartt et al. 2009; Bersten et al. 2011 and references therein). As a result, only approximate values of the physical parameters can be derived using these relations. Fortunately, the observed parameters are derived very accurately for SN 2008in. The Δt_p is $\sim$98 days (Section 3.2), the v_{mp} is 2694 ± 70[27] $\mathrm{km \, s^{-1}}$, and the M_{Vmp} is estimated as -15.32 ± 0.38 mag.[28] Now, employing analytical relations, we estimate $E_0 \sim 0.54$ foe, $M_{\mathrm{ej}} \sim 16.7 \, M_{\odot}$, and $R_0 \sim 127 \, R_{\odot}$. The explosion energy derived in this way is consistent with that predicted from the hydrodynamical simulations of the ejecta kinematics.

---

[27] This is the mean value of the velocities computed from the lines of Fe II λ4924, λ5018, and λ5169 in the +54 day spectrum.
[28] These observed values of M_{Vmp} and v_{mp} can be compared with the estimates derived empirically between the mass of ^{56}Ni, and the v_{mp} and M_{Vmp} for a larger sample of IIP SNe (see Section 8.3 of Roy et al. 2011). Using the ^{56}Ni mass of $0.015 \pm 0.003 \, M_{\odot}$ we find $v_{\mathrm{mp}} = 2916 \pm 220 \, \mathrm{km \, s^{-1}}$ and $M_{\mathrm{Vmp}} = -15.37 \pm 0.23$ mag, which are consistent with those measured observationally.
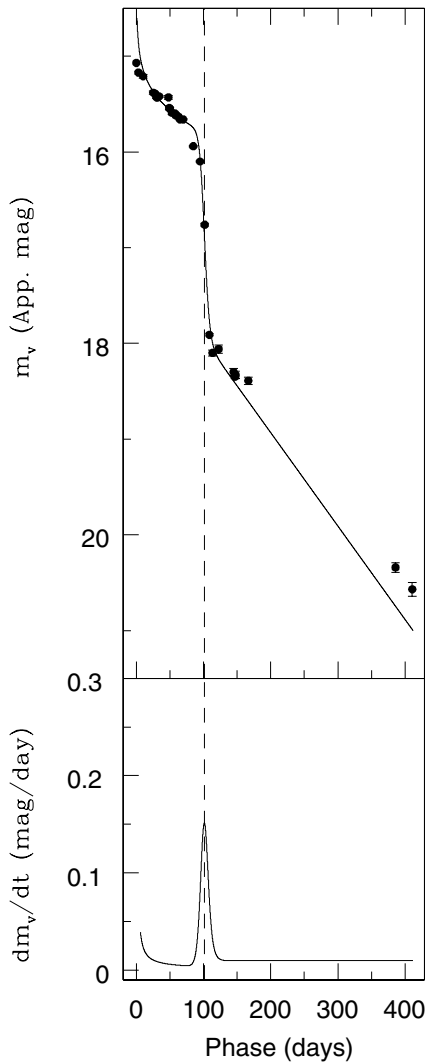
Figure 13. Determination of the steepness parameter from the apparent *V*-band light curve of SN 2008in. See the text for details.

The explosion energy of SN 2008in indicates that the event was less energetic than the standard IIP SNe 1999em, 2004et and more energetic than SN 2005cs. Assuming a net mass loss of $\sim$0.5 $M_\odot$ due to stellar wind[29] and accounting for a compact remnant with mass $\sim$1.5–2 $M_\odot$ (Sahu et al. 2006), we find the initial mass of the progenitor to be $\leqslant$20 $M_\odot$.

8. DISCUSSION IN CONTEXT OF OTHER TYPE IIP SNe

In Figure 14, we compare the light curve of SN 2008in in absolute *V*-band magnitude with a sample of 13 other well-studied Type II SNe taken from the literature (see Misra et al. 2007 and Roy et al. 2011 for the references). The sample includes two low-luminosity Type IIP SNe 1997D, 2005cs; nine normal Type IIP SNe 1990E, 1992H, 1999gi, 1999em, 2003gd, 2004A, 2004dj, 2004et, 2008gz, and two peculiar Type II SNe 1987A, 1998A. It is seen that the Type II SNe show a wide range of mid-plateau luminosity, i.e., from -14 to -17 mag. The data

---

[29] SN 2008in was not detected in X-rays. The lack of X-ray emission can be used to constrain the mass-loss rate of the progenitor system that could be heated by the outgoing shock to X-ray emitting temperatures. Following the discussion in Immler et al. (2007) and references therein, an upper limit to the pre-SN mass-loss rate of $5 \times 10^{-6}\ M_\odot\ \mathrm{yr}^{-1}\ (v_\mathrm{w}/10\ \mathrm{km\,s}^{-1})$ with an uncertainty of a factor of two to three is obtained.

on low-luminosity SNe (see also Table 4 in Pastorello et al. 2006) indicate that their M_{Vmp} lie between -14 and -15 mag, with the only exception of SN 2002gd, whereas the other SNe are seen to lie between -16 and -17 mag. With the M_{Vmp} of -15.32 mag,[30] the SN 2008in presents another case which occupies the gap between low and normal luminosity Type IIP events.

The tail luminosity is an important indication of ejected nickel mass. The average tail luminosity of SN 2008in ($M_\mathrm{v} \sim -12.16$) is nearly 2.3 mag brighter than those of the low-luminosity SNe 1997D and 2005cs ($\sim$$-9.6$ mag), and about 1.3 mag fainter than the normal Type IIP SNe 1992H, 2004et, and 2008gz ($\sim$$-13.5$ mag). A close inspection shows that the average tail luminosity of SN 2008in is roughly similar to Type IIP SNe 2004dj in NGC 2403 and 2003gd in M74, whereas their plateau is brighter ($\sim$0.5–0.8 mag at mid-plateau) than SN 2008in. These comparisons of nebular phase luminosities with other SNe are consistent with a quite modest radioactive ^{56}Ni production for SN 2008in (Section 7.1).

The luminosity and shape of the tail depend on the ^{56}Ni mass and the radiant energy per unit ejected mass (E/M_ej). The first parameter determines the absolute magnitude, while the second determines its decay rate (see Turatto et al. 1998 and references therein). The measured values of ejected ^{56}Ni mass for SNe 2003gd, 2004dj, and 2008in are, respectively, $\sim$0.016 (Hendry et al. 2005), 0.017 (Vinkó et al. 2006), and 0.015 $M_\odot$. These are more than twice the ^{56}Ni amount synthesized by the low-luminosity SNe 1997D ($\sim$0.002 $M_\odot$; Turatto et al. 1998) and 2005cs (0.003–0.004 $M_\odot$; Pastorello et al. 2009), although at least three times less than the ^{56}Ni produced by normal Type IIP SNe such as 1992H ($\sim$0.075 $M_\odot$; Clocchiatti et al. 1996), 2004et ($\sim$0.06 $M_\odot$; Sahu et al. 2006; Maguire et al. 2010), and 2008gz ($\sim$0.05 $M_\odot$; Roy et al. 2011). Similarly, the measured value of the E/M_ej ratio for SN 2008in is larger than that for the low-luminosity SN 1997D and lower than other Type IIP events.[31]

Though we have an approximate value of the pre-SN radius (128 $R_\odot$), it can be seen that the progenitor radius of SN 2008in is smaller than or comparable to that of low-luminosity SNe 1997D ($\sim$300 $R_\odot$; Turatto et al. 1998), 2005cs (100–600 $R_\odot$; Pastorello et al. 2009; Utrobin & Chugai 2008), 1999br (114 $R_\odot$; Zampieri et al. 2003) and much smaller than that of normal Type IIP SNe like 1992H (>600 $R_\odot$; Clocchiatti et al. 1996), 2004et ($\sim$530 $R_\odot$; Misra et al. 2007). We also note that the SN 2008in progenitor is only slightly larger than the blue supergiant progenitors of SNe 1987A and 1998A (Pastorello et al. 2005).
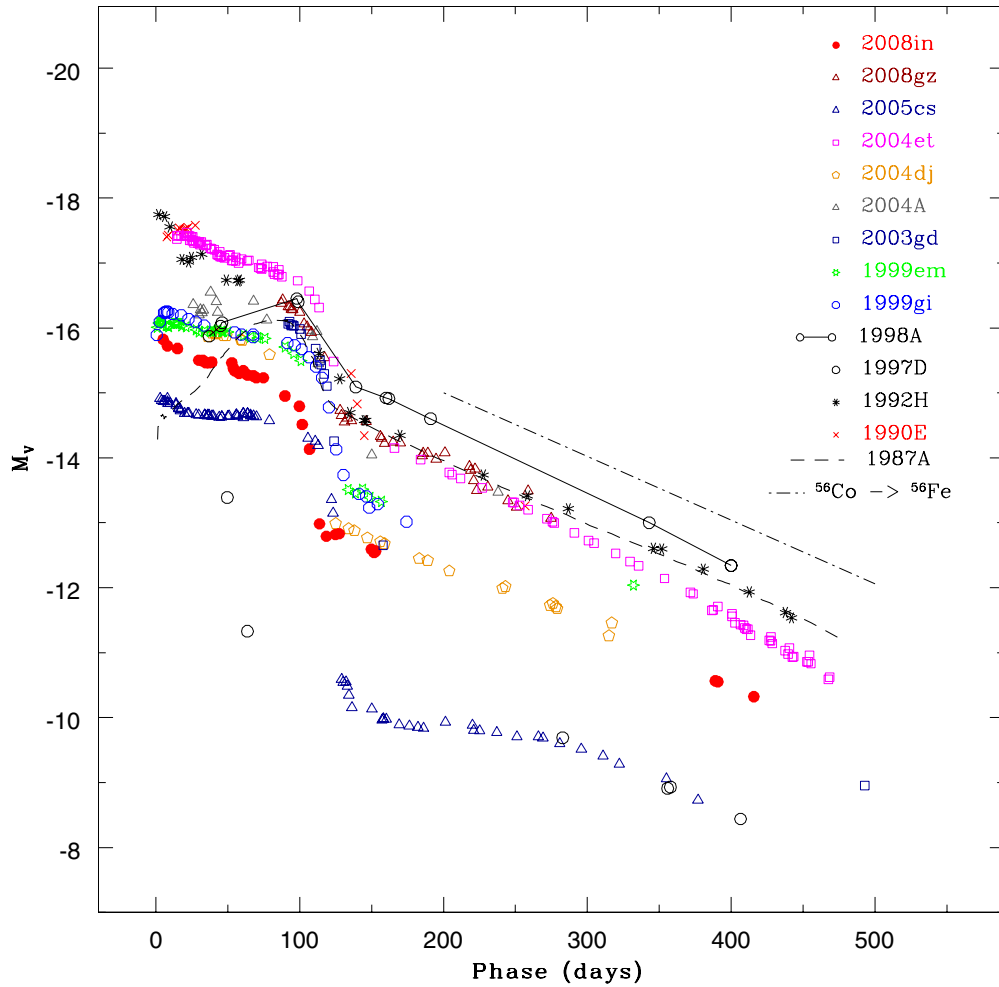
Information about the metallicity of the SNe location is essential to constrain the triggering mechanism of the SN explosion (Heger et al. 2003). The oxygen abundance [O/H] of SN 2008in is about 8.44 dex[32] which is marginally lower than

---

[30] Considering a lower value of $A_V = 0.139 \pm 0.002$, we get $M_{\mathrm{Vmp}} = -15.1 \pm 0.2$.

[31] The measured value of the E/M ratio for SN 2008in is 3.5×10^{49} erg $M_\odot^{-1}$, which is twice the E/M ratio measured for SNe 1997D (1.7×10^{49} erg $M_\odot^{-1}$; Turatto et al. 1998), but it is half those of SN 2008gz (7.3×10^{49} erg $M_\odot^{-1}$; Roy et al. 2011), SN 2004dj (7.3×10^{49} erg $M_\odot^{-1}$; Vinkó et al. 2006), and SN 2004et (7.5×10^{49} erg $M_\odot^{-1}$; Sahu et al. 2006). Finally, it is barely a third the E/M ratios of SNe 1987A (11.3×10^{49} erg $M_\odot^{-1}$; Hamuy 2003) and 2003gd (13.0×10^{49} erg $M_\odot^{-1}$; Hendry et al. 2005), and about seven times smaller than a luminous event like SN 1998A (25.4×10^{49} erg $M_\odot^{-1}$; Pastorello et al. 2005).

[32] Derived from the [O/H]($=12 + \log(N_\mathrm{O}/N_\mathrm{H})$)–$M_B$ relation given by Pilyugin et al. (2004) for a given deprojected radius and galaxy type. The host of SN 2008in is a spiral galaxy of SBbc Type and the SN location is $\sim$1$\farcs$8

Figure 14. Comparison of the absolute *V*-band light curve of SN 2008in with the low-luminosity SNe 1997D, 2005cs; the normal SNe 1999em, 2004et, 2008gz, 2004dj, 2004A, 2003gd, 19992H, 1999E, and 1999gi; and the peculiar Type II SNe 1987A and 1998A. The decline rate of emission expected from radioactive decay of ^{56}Ni to ^{56}Co to ^{56}Fe is shown with the dot-dashed line.

(A color version of this figure is available in the online journal.)

the solar value of 8.65 dex (Asplund et al. 2009). A comparison[33] of [O/H] of all the events in our sample indicates that there is no clear trend in the type of event and the metallicity.

The photometric and spectroscopic comparisons of SN 2008in with some Type II SNe covering a wide range of physical parameters put observational constraints on the nature of the progenitor of this event, pointing toward a star that was more compact than a typical M-type red supergiant, and closer to a blue supergiant, maybe a yellow supergiant. However, the direct detection of the progenitors of a few faint SNe IIP in pre-explosion archive *Hubble Space Telescope* images seems to contradict this conclusion (see Smartt et al. 2009 for a review). Our spectroscopic study suggests that in SN 2008in the hydrogen envelope ejected by the explosion is smaller than in most Type II events but larger than that ejected in low-luminosity

events (such as SN 1997D, SN 1999br, and SN 1999eu). This may be due to a significant mass loss of the parent star in the latest stages of its life. This conclusion is also partially supported by the upper limit mass-loss rate of the progenitor revealed from the X-ray study (Section 7.2). In view of the upper mass limit of a 20 $M_\odot$ progenitor, occurrence of the event in a sub-solar metallicity region, and following the evolution of a single massive star as a function of metallicity (Heger et al. 2003), we rule out the possibility of a "fall back of ejecta to BH" scenario in the case of SN 2008in, supporting the scenario of a weak explosion of a relatively compact progenitor.

9. CONCLUSION

Low-luminosity Type IIP SNe belong to a poorly known class of events due to the unknown nature of their progenitors as well as the explosion mechanism. Spectroscopic as well as photometric characteristics of these events are significantly different from the normal and peculiar Type IIP SNe. The number of such underluminous events discovered so far is relatively small. This could plausibly be a selection effect. If we confine the search of core-collapse SNe to a small volume, the majority of SNe discovered in the local universe are of Type IIP (~48.2%; Smith et al. 2010) and probably a large fraction of them would turn out to be underluminous. Incidentally

---

away from the center of the host. This corresponds to a deprojected distance ~7.03 kpc.

[33] We have taken the [O/H] value from Smartt et al. (2009), though for a few cases the values are estimated using the [O/H]−M_B relation mentioned in Pilyugin et al. (2004). The [O/H] for normal Type IIP SNe 2008gz, 1999em and low-luminosity SNe 1999eu, 2005cs is about 8.6. For the low-luminosity SNe 1994N, 1999br, 2001dc, 2003gd, 2004dj, 1997D, and the normal SN 2004et, it is about 8.4. In many cases, we have adopted the [O/H] value from Smartt et al. (2009). For some cases we have estimated the value by adopting the [O/H]−M_B relation mentioned in Pilyugin et al. (2004).

SN 1999br, SN 2005cs, and SN 2009md are the only events of this group to have been discovered soon after the core-collapse and whose data are publicly available.

In this study, we have reported the results of an extensive photometric and spectroscopic follow-up campaign for SN 2008in in the ultraviolet, optical, and near-infrared domains. The SN was also observed (although not detected) at X-ray and radio wavelengths. The SN was observed soon after its explosion, during the fast rise of the light curve to the optical maximum. Evidence for a shock breakout in SN 2008in was primarily derived through the analysis of the ROTSE-IIIb R-band light curve. An upper limit of 16.16 mag in the R band was estimated about two days before the discovery.

Modeling the R-band light curve allowed us to estimate a reliable epoch of the shock breakout, with an uncertainty of about two days. The plateau phase in SN 2008in lasts about 98 days, which is marginally shorter than in normal Type IIP SNe. The evolution of the bolometric light curve indicates that the event is somewhat in between the normal and faint Type IIP events. The luminosity of the nebular phase light curve indicates an ejected ^{56}Ni mass of $\sim 0.015\,M_\odot$, a factor two higher than that derived for low-luminosity IIP SNe. The spectroscopic evolution of SN 2008in is similar to those of low-luminosity IIP SNe (1997D, 1999br, and 1999eu), indicated particularly by the strong presence of Ba II lines, the narrow line widths of Hα lines, and the expansion velocities of SN during the photospheric phases ($\sim 3000\,\mathrm{km\,s^{-1}}$) and the nebular phases ($\sim 1200\,\mathrm{km\,s^{-1}}$). The ejecta kinematics of SN 2008in are consistent with less-energetic ($\sim 5 \times 10^{50}$ erg) Type IIP SNe.

Spectroscopically SN 2008in appears to be like low-luminosity SNe IIP, but photometrically it appears close to a normal type IIP event.

From the light curve and spectra of SN 2008in, we could determine quite accurate values of the observed properties such as plateau duration, mid-plateau luminosity as well as the photospheric velocity, and this has helped us to comment on the properties of the explosion and the progenitor star. Using semi-analytical formulae by Litvinova & Nadezhin (1985), we could estimate approximate values of the explosion energy $\sim 5.4 \times 10^{50}$ erg, the ejected mass $\sim 17\,M_\odot$, and the pre-SN radius $\sim 127\,R_\odot$. The explosion energy of SN 2008in is smaller than the normal ($\geqslant 10^{51}$ erg) Type IIP events, although higher than that estimated in underenergetic ($\sim 10^{50}$ erg) SNe IIP. We could provide an upper limit to the mass-loss rate of the progenitor as $5 \times 10^{-6}\,M_\odot\,\mathrm{yr^{-1}}(v_\mathrm{w}/10\,\mathrm{km\,s^{-1}})$ whereas the upper limit for the main-sequence mass of the progenitor star is estimated as $20\,M_\odot$.

REFERENCES

Akerlof, C. W., et al. 2003, PASP, 115, 132

Alard, C. 2000, A&AS, 144, 363

Arnett, W. D. 1980, ApJ, 237, 541

Arnett, W. D. 1996, Supernovae and Nucleosynthesis: An Investigation of the History of Matter, from the Big Bang to the Present (Princeton, NJ: Princeton Univ. Press)

Asplund, M., Grevesse, N., Sauval, A. J., & Scott, P. 2009, ARA&A, 47, 481

Barbon, R., Benetti, S., Rosino, L., Cappellaro, E., & Turatto, M. 1990, A&A, 237, 79

Benetti, S., et al. 2001, MNRAS, 322, 361

Bersten, M. C., Benvenuto, O., & Hamuy, M. 2011, ApJ, 729, 61

Bessell, M. S., Castelli, F., & Plez, B. 1998, A&A, 333, 231

Brown, P. J. 2009, PhD thesis, Pennsylvania State Univ.

Brown, P. J., et al. 2009, AJ, 137, 4517

Burrows, D. N., et al. 2005, Space Sci. Rev., 120, 165

Chakraborti, S., Prabhu, T., Anupama, G. C., Kaur, A., Uday Kumar, G., & Ray, A. 2008, CBET, 1638, 1

Chevalier, R. A. 1976, ApJ, 207, 872

Chugai, N. N., & Utrobin, V. P. 2000, A&A, 354, 557

Clocchiatti, A., et al. 1996, AJ, 111, 1286

Cowen, D. F., Franckowiak, A., & Kowalski, M. 2010, Astropart. Phys., 33, 19

Dessart, L., Livne, E., & Waldman, R. 2010, MNRAS, 408, 827

Dickey, J. M., & Lockman, F. J. 1990, ARA&A, 28, 215

Eldridge, J. J., Mattila, S., & Smartt, S. J. 2007, MNRAS, 376, L52

Eldridge, J. J., & Tout, C. A. 2004, MNRAS, 353, 87

Elmhamdi, A., Chugai, N. N., & Danziger, I. J. 2003a, A&A, 404, 1077

Elmhamdi, A., et al. 2003b, MNRAS, 338, 939

Falk, S. W., & Arnett, W. D. 1977, ApJS, 33, 515

Foley, R. J. 2008, CBET, 1638, 2

Fransson, C., & Chevalier, R. A. 1987, ApJ, 322, L15

Fransson, C., Lundqvist, P., & Chevalier, R. A. 1996, ApJ, 461, 993

Fraser, M., et al. 2010, arXiv:1011.6558

Gezari, S., et al. 2008, ApJ, 683, L131

Grassberg, E. K., Imshennik, V. S., & Nadyozhin, D. K. 1971, Ap&SS, 10, 28

Hamuy, M. 2003, ApJ, 582, 905

Hamuy, M. 2005, in IAU Colloq. 192, Cosmic Explosions, On the 10th Anniversary of SN1993J, ed. J.-M. Marcaide & K. W. Weiler (Berlin: Springer), 535

Hamuy, M., & Pinto, P. A. 2002, ApJ, 566, L63

Hamuy, M., Suntzeff, N. B., Heathcote, S. R., Walker, A. R., Gigoux, P., & Phillips, M. M. 1994, PASP, 106, 566

Hamuy, M. 2001, PhD thesis, Univ. Arizona

Heger, A., Fryer, C. L., Woosley, S. E., Langer, N., & Hartmann, D. H. 2003, ApJ, 591, 288

Hendry, M. A., et al. 2005, MNRAS, 359, 906

Immler, S., et al. 2007, ApJ, 664, 435

Landolt, A. U. 2009, AJ, 137, 4186

Leonard, D. C., et al. 2002, PASP, 114, 35

Litvinova, I. Y., & Nadezhin, D. K. 1985, Sov. Astron. Lett., 11, 145

Maguire, K., et al. 2010, MNRAS, 404, 981

Maund, J. R., & Smartt, S. J. 2005, MNRAS, 360, 288

Maund, J. R., Smartt, S. J., & Danziger, I. J. 2005, MNRAS, 364, L33

Misra, K., Pooley, D., Chandra, P., Bhattacharya, D., Ray, A. K., Sagar, R., & Lewin, W. H. G. 2007, MNRAS, 381, 280

Nadyozhin, D. K. 2003, MNRAS, 346, 97

Nakano, S., Kadota, K., & Wells, W. 2008, CBET, 1636, 1

Olivares, E. F., et al. 2010, ApJ, 715, 833

Pastorello, A., et al. 2004, MNRAS, 347, 74

Pastorello, A., et al. 2005, MNRAS, 360, 950
Pastorello, A., et al. 2006, MNRAS, 370, 1752
Pastorello, A., et al. 2009, MNRAS, 394, 2266
Pilyugin, L. S., Vílchez, J. M., & Contini, T. 2004, A&A, 425, 849
Poole, T. S., et al. 2008, MNRAS, 383, 627
Press, W. H., Teukolsky, S. A., Vetterling, W. T., & Flannery, B. P. (ed.) 1992, in Numerical Recipes in C. The Art of Scientific Computing (Cambridge: Cambridge Univ. Press)
Quimby, R. M., Wheeler, J. C., Höflich, P., Akerlof, C. W., Brown, P. J., & Rykoff, E. S. 2007, ApJ, 666, 1093
Richmond, M. W., Treffers, R. R., Filippenko, A. V., Paik, Y., Leibundgut, B., Schulman, E., & Cox, C. V. 1994, AJ, 107, 1022
Roming, P. W. A., et al. 2005, Space Sci. Rev., 120, 95
Roy, R., et al. 2011, MNRAS, 414, 167
Sahu, D. K., Anupama, G. C., Srividya, S., & Muneer, S. 2006, MNRAS, 372, 1315
Schawinski, K., et al. 2008, Science, 321, 223
Schlegel, D. J., Finkbeiner, D. P., & Davis, M. 1998, ApJ, 500, 525
Smartt, S. J., Eldridge, J. J., Crockett, R. M., & Maund, J. R. 2009, MNRAS, 395, 1409
Smith, N., Li, W., Filippenko, A. V., & Chornock, R. 2011, MNRAS, 412, 1522
Stetson, P. B. 1987, PASP, 99, 191
Stockdale, C. J., et al. 2008, ATel, 1883, 1
Stockdale, C. J., et al. 2009, ATel, 1912, 1

Stritzinger, M. 2008, CBET, 1638, 3
Suntzeff, N. B., & Bouchet, P. 1990, AJ, 99, 650
Terry, J. N., Paturel, G., & Ekholm, T. 2002, A&A, 393, 57
Tominaga, N., Blinnikov, S., Baklanov, P., Morokuma, T., Nomoto, K., & Suzuki, T. 2009, ApJ, 705, L10
Turatto, M., Benetti, S., & Cappellaro, E. 2003, in Proc. ESO/MPA/MPE, From Twilight to Highlight: The Physics of Supernovae, ed. W. Hillebrandt & B. Leibundgut (Berlin: Springer), 200
Turatto, M., et al. 1998, ApJ, 498, L129
Utrobin, V. P. 2007, A&A, 461, 233
Utrobin, V. P., & Chugai, N. N. 2008, A&A, 491, 507
Utrobin, V. P., Chugai, N. N., & Botticella, M. T. 2010, ApJ, 723, L89
van Dokkum, P. G. 2001, PASP, 113, 1420
Van Dyk, S. D., et al. 2010, arXiv:1011.5873
Vinkó, J., et al. 2006, MNRAS, 369, 1780
Vollmann, K., & Eversberg, T. 2006, Astron. Nachr., 327, 862
Waxman, E., Mészáros, P., & Campana, S. 2007, ApJ, 667, 351
Weiler, K. W., Panagia, N., Montes, M. J., & Sramek, R. A. 2002, ARA&A, 40, 387
Yuan, F. 2010, PhD thesis, Univ. Michigan
Zampieri, L., Pastorello, A., Turatto, M., Cappellaro, E., Benetti, S., Altavilla, G., Mazzali, P., & Hamuy, M. 2003, MNRAS, 338, 711
Zampieri, L., Shapiro, S. L., & Colpi, M. 1998, ApJ, 502, L149
Zerbi, F. M., et al. 2004, Proc. SPIE, 5492, 1590